UNIVERSITÀ DEGLI STUDI DI PADOVA

Dipartimento di Fisica e Astronomia "Galileo Galilei"

Master Degree in Astrophysics and Cosmology

Final Dissertation

A Common Origin for WIMP Dark Matter and the Baryon Asymmetry of the Universe

Thesis supervisor

Prof. Francesco D'Eramo

Candidate

Tullia Girardi

Academic Year 2024/2025

Abstract

The Standard Model of particle physics, despite its remarkable success, fails to explain two key phenomena in cosmology: the nature of dark matter (DM) and the baryon asymmetry of the Universe. These two issues highlight the need for physics beyond the SM. Weakly Interacting Massive Particles (WIMPs) have long been considered among the main candidates for DM due to the so-called "WIMPs miracle", by which their relic abundance naturally matches the observed dark matter density. On the other hand, the Sakharov conditions provide a theoretical framework for generating the baryon asymmetry, through a Baryogenesis process, although their realization often requires extensions to the SM.

This thesis explores the interesting possibility of a unified solution to these problems via a "WIMPy Baryogenesis". This mechanism proposes that WIMPs annihilations satisfy the Sakharov conditions, generating a baryon asymmetry besides producing the dark matter relic density.

The theoretical framework is developed through Boltzmann equations describing particle number densities and asymmetry evolution. It is shown the importance of the freeze-out moment of the washout processes in order to get the expected baryon asymmetry, which translates into a relation between the masses involved. It is proposed one possible model in which WIMPs annihilate directly into quarks, plus a new massive baryon field. Finally, the main dependencies of the final value of the asymmetry are analyzed.

Contents

1 Introduction to the Standard Model **1**
1.1 Theoretical Construction of the Standard Model 2
1.1.1 Gauge Group and Quantum Numbers of Particles 2
1.1.2 The Standard Model Lagrangian 3
1.1.3 Electroweak Interactions 5
1.1.4 Strong Interactions 6
1.1.5 Spontaneous Electroweak Symmetry Breaking 6
1.1.6 Fermion Masses 7
1.2 Successes of the Standard Model 8
1.3 Limitations of the Standard Model 10
1.4 Conclusion 13

2 Baryogenesis **15**
2.1 Matter-Antimatter Asymmetry 15
2.1.1 Observational Evidence 15
2.1.2 Implications for the Matter-Antimatter Asymmetry 17
2.2 Baryogenesis model 18
2.2.1 Sakharov conditions 18
2.2.2 Sakharov Conditions in the Standard Model and Electroweak Baryogenesis 20
2.2.3 Toy model 22
2.3 Conclusion 26

3 Dark Matter **27**
3.1 Evidences for Dark Matter 27
3.1.1 Galactic Scale Evidence 28
3.1.2 Evidence from Galaxy Clusters 28
3.1.3 Cosmological scale evidence 29

3.1.4 Numerical simulations 29
3.2 WIMPs as Dark Matter Candidates 29
3.2.1 Boltzmann equations for WIMPs 30
3.3 Conclusion 35

4 WIMPy Baryogenesis **39**
4.1 General theory 40
4.2 Baryon asymmetry expectations 43
4.3 Model of WIMP Annihilation to Quarks 47
4.3.1 Overview 48
4.3.2 Generation of the asymmetry and washout processes . . . 50
4.3.3 Numerical analysis: evolution of abundances and parameters dependence 55

5 Conclusions and Future Works **59**

A Standard Model of Cosmology **63**
A.1 Friedmann equations 63
A.2 Equilibrium thermodynamics 66

B Boltzmann equations **69**
B.1 Boltzmann equations for Baryogenesis 71
B.2 Boltzmann equations for WIMPs 76
B.3 Boltzmann equations for WIMPy Baryogenesis 78

C Cross Section Evaluation **81**
C.1 WIMPs annihilation cross section 81
C.2 Scattering cross-section 83

References **87**

1

Introduction to the Standard Model

The first chapter introduces the Standard Model of particle physics, the theoretical framework that currently better describes the fundamental particles and their interactions.

In Section 1.1 we will guide the reader through the theoretical construction of the Standard Model and its core concepts, starting from its gauge group structure and the quantum numbers of particles. We will then present and discuss the Standard Model Lagrangian and the fundamental interactions that it describes: the electroweak and strong interactions, the Yukawa couplings, and the spontaneous symmetry breaking mechanism that gives rise to the masses of the W and Z bosons.

Section 1.2 will be dedicated to the experimental successes of the Standard Model, highlighting the key discoveries that have confirmed its validity. Particular attention will be given to the discovery of the Higgs boson, which provided experimental evidence for the Higgs mechanism.

Finally, in Section 1.3, we will explore the limitations of the Standard Model. Despite its numerous successes, the model leaves several fundamental questions unanswered. We will discuss issues such as the nature of dark matter, baryogenesis, the strong CP problem, the gauge hierarchy problem, the mass of neutrinos, the grand unification, and the mystery of dark energy. These open questions point to the need for physics beyond the Standard Model and set the stage for exploring new theoretical frameworks in the subsequent chapters of this thesis.

1.1 Theoretical Construction of the Standard Model

1.1.1 Gauge Group and Quantum Numbers of Particles

The SM is built on the symmetry group $SU(3)_C \times SU(2)_L \times U(1)_Y$, which describes the strong and the electroweak interactions. Elementary particles, such as quarks and leptons, are classified according to their representations under these gauge groups, defined by quantum numbers.

In the SM, particles are divided into two main categories:

- **Fermions**, which include quarks and leptons. These particles are grouped into three families, each consisting of two quarks (one with electric charge +2/3 and one with charge −1/3) and two leptons (one with charge −1 and a neutral neutrino).

  Particles have in common with their equivalents inside different families the same properties except for the value of the mass.

$$1^{st} \text{ family: } \begin{pmatrix} \nu_e \\ e^- \end{pmatrix}_L, e_R^-, \begin{pmatrix} u \\ d \end{pmatrix}_L, u_R, d_R$$

$$2^{nd} \text{ family: } \begin{pmatrix} \nu_\mu \\ \mu^- \end{pmatrix}_L, \mu_R^-, \begin{pmatrix} c \\ s \end{pmatrix}_L, c_R, s_R$$

$$3^{rd} \text{ family: } \begin{pmatrix} \nu_\tau \\ \tau^- \end{pmatrix}_L, \tau_R^-, \begin{pmatrix} t \\ b \end{pmatrix}_L, t_R, b_R$$

  The left-handed and right-handed particles are defined as[1]:

$$e_L^- = \frac{1}{2}(1 - \gamma_5)e^-, e_R^- = \frac{1}{2}(1 + \gamma_5)e^- \tag{1.1}$$

  and they transform as doublets and singlets of $SU(2)_L$ respectively.

[1] $\gamma^5 \equiv i\gamma^0\gamma^1\gamma^2\gamma^3$. In Chiral representation these matrices are:

$$\gamma^\mu = \begin{bmatrix} 0 & \sigma^\mu \\ \bar{\sigma}^\mu & 0 \end{bmatrix}$$

where $\sigma^\mu = (1, \sigma^i)$, $\bar{\sigma}^\mu = (1, -\sigma^i)$ and σ^i stand for the Pauli matrices.

- **Bosons**, which include the gauge bosons that mediate the fundamental interactions: the gluons (g) for the strong interaction, the $W^{\pm}$ and Z bosons for the weak interaction, and the photon (γ) for the electromagnetic interaction; and one scalar boson, the Higgs, which is responsible for the spontaneous breaking of the electroweak symmetry.

Each fermion carries quantum numbers (see tables 1.1, 1.2) that determine the way in which it couples with gauge fields:

- Color charge associated to ($SU(3)_C$), that governs strong interactions.
- Weak isospin associated to ($SU(2)_L$), that determines how the particles participate to weak interactions.
- Hypercharge associated to ($U(1)_Y$), that determines the electric charge of particles via the relation $Q = T_3 + Y/2$, where T_3 is the third component of weak isospin.

Lepton	$SU(3)_C$	T_3	Y	Q
ν_{e_L}	0	1/2	-1	0
e_L^-	0	-1/2	-1	-1
e_R^-	0	0	-2	-1

Table 1.1: Lepton quantum numbers

Quark	$SU(3)_C$	T_3	Y	Q
u_L	3	1/2	1/3	2/3
d_L	3	-1/2	1/3	-1/3
u_R	3	0	4/3	2/3
d_R	3	0	-2/3	-1/3

Table 1.2: Quarks quantum numbers

1.1.2 The Standard Model Lagrangian

The dynamics of particles in the SM are described by a Lagrangian that is invariant under the transformations of the $SU(3)_C \times SU(2)_L \times U(1)_Y$ gauge group. The SM Lagrangian can be divided into four main components:

$$\mathcal{L}_{SM} = \mathcal{L}_{gauge} + \mathcal{L}_{matter} + \mathcal{L}_{Yukawa} + \mathcal{L}_{Higgs}, \tag{1.2}$$

where:

- $\mathcal{L}_{gauge}$ describes the dynamics of the gauge fields ($G^a_{\mu\nu}$, $W^i_{\mu\nu}$, and $B_{\mu\nu}$):

$$\mathcal{L}_{gauge} = -\frac{1}{4}G^a_{\mu\nu}G^{a\mu\nu} - \frac{1}{4}W^i_{\mu\nu}W^{i\mu\nu} - \frac{1}{4}B_{\mu\nu}B^{\mu\nu}. \tag{1.3}$$

  These terms include self-interactions of gauge bosons for the non-Abelian sectors $SU(3)_C$ and $SU(2)_L$. For example gluons interact with other gluons, which can be seen in the last term of the field (it gives a quartic term in the Lagrangian):

$$G^a_{\mu\nu} = \partial_\mu G^a_\nu - \partial_\nu G^a_\mu + g_s f^{abc} G^b_\mu G^c_\nu, \tag{1.4}$$

  where f^{abc} are structure constants of $SU(3)_C$ e g_s is the strong coupling constant.

- $\mathcal{L}_{matter}$ describes the kinetic of fermions and their interactions with the gauge fields:

$$\mathcal{L}_{matter} = i\bar{\psi}_L \not{D} \psi_L + i\bar{\psi}_R \not{D} \psi_R. \tag{1.5}$$

  Fermions couple with gauge fields according to their quantum numbers through the covariant derivative:

$$D_\mu = \partial_\mu - ig_s T^a G^a_\mu - igT^i W^i_\mu - ig' Y B_\mu, \tag{1.6}$$

  with T^a and T^i being the generators for the $SU(3)_C$ and $SU(2)_L$ groups, and Y the hypercharge associated with $U(1)_Y$.

- $\mathcal{L}_{Yukawa}$ describes the Yukawa interactions:

$$\mathcal{L}_{Yukawa} = -\sum_{i,j} Y_{ij}\bar{\psi}_{i,L}\Phi\psi_{j,R} + \text{h.c.}^{2} \tag{1.7}$$

  where Y_{ij} are the Yukawa couplings that govern the strength of the interaction between left-handed fermions $\psi_{i,L}$, right-handed fermions $\psi_{j,R}$, and the Higgs field Φ. This term is responsible for giving mass to fermions via the Higgs mechanism. The details of this process will be addressed in Section 1.1.6.

[2]h.c. is the hermitian conjugate.

- $\mathcal{L}_{Higgs}$ describes the Higgs field and its dynamics, that brings to the spontaneous breaking of the electroweak symmetry and the generation of masses for the W and Z bosons (discussed in Section 1.1.5):

$$\mathcal{L}_{Higgs} = |D_\mu \Phi|^2 - V(\Phi), \tag{1.8}$$

where D_μ is the covariant derivative involving the electroweak gauge fields, and $V(\Phi)$ is the Higgs potential that triggers spontaneous symmetry breaking when the field acquires a non-zero vev:

$$V(\Phi) = \mu^2|\Phi|^2 + \lambda|\Phi|^4. \tag{1.9}$$

1.1.3 Electroweak Interactions

The electroweak interactions in the SM are described by the $SU(2)_L \times U(1)_Y$ gauge group. The spontaneous breaking of the electroweak symmetry via the Higgs mechanism results in the combination of the W^i_μ and B_μ fields to form the physical $W^\pm$, Z and photon (γ) bosons, that are the mediators of the weak and electromagnetic interactions.

The weak interactions involve both charged current and neutral current interactions: charged current interactions, mediated by the $W^\pm$ bosons, are responsible for processes such as beta decay, while neutral current interactions, mediated by the Z boson, regulate processes such as neutrino scattering.

Fermions couple differently to the gauge bosons depending on their quantum numbers. For instance:

- Charged leptons (e.g. the electron) couple to the photon, Z, and $W^\pm$ bosons.
- Neutrinos interact only via the Z and $W^\pm$ bosons.
- Quarks couple to messengers of all the interactions: strong (gluons), electromagnetic (photon), and weak (W, Z).

The two interactions descending from the electroweak one, at our energies, are characterized by very different strengths. The electromagnetic interactions are governed by the size of the electromagnetic coupling constant through $\alpha = \frac{e^2}{4\pi}$, which at low energies is given by the fine structure constant, $\alpha(Q = m_e) = \frac{1}{137}$. The weak interactions strength instead, at low energies (that here means lower than M_W), is of the order of the Fermi constant $G_F = 1.167 \cdot 10^{-5} GeV^{-2}$, which motivates their name.

1.1.4 Strong Interactions

The strong interactions are described by the $SU(3)_C$ gauge group, and mediated by gluons (there are N^2 - 1 = 8 of them).

Quarks carry a color charge and interact strongly via gluon exchange. At our energies, strong interaction shows a peculiar property: quarks are never observed as free particles but they are always confined inside hadrons, such as protons and neutrons, which are overall colorless particles (color confinement).

In terms of strength of the coupling, the strong interaction gets its name from the value it takes at low energies: $\alpha_S(Q = m_{hadron}) \approx 1$, with $\alpha_S = \frac{g_S^2}{4\pi}$. However, this value decreases at increasing energies, up to the asymptotic limit at which it vanishes, so that hypotetically quarks would be allowed to behave almost as free particles (asymptotic freedom).

1.1.5 Spontaneous Electroweak Symmetry Breaking

Spontaneous electroweak symmetry breaking occurs when the Higgs field acquires a non-zero vev, breaking the $SU(2)_L \times U(1)_Y$ symmetry down to $U(1)_{\text{em}}$. This process gives mass to the $W^\pm$ and Z^0 bosons, while the photon remains massless.

The Higgs potential, $V(\Phi) = \mu^2|\Phi|^2 + \lambda|\Phi|^4$, causes the symmetry breaking when $\mu^2 < 0$, resulting in the Higgs field acquiring the vev:

$$\langle\Phi\rangle = \frac{v}{\sqrt{2}}, \tag{1.10}$$

with $v \approx 246\,\text{GeV}$.

When there is a symmetry breaking, for each generator of the symmetry we have an unphysical Goldostone boson, which plays the role of the longitudinal polarization of the vector boson: in this way it gains a mass.

After the symmetry breaking, the masses of the W and Z bosons are given by:

$$m_W = \frac{gv}{2}, \tag{1.11}$$

$$m_Z = \frac{\sqrt{g^2 + g'^2}v}{2}, \tag{1.12}$$

where g and g' are the coupling constants of $SU(2)_L$ and $U(1)_Y$, respectively. The photon instead remains massless because there is a residual gauge symmetry, that is $U(1)_{\text{em}}$.

1.1.6 Fermion Masses

Fermions acquire mass via the Yukawa mechanism, in which they interact with the Higgs field through the Yukawa Lagrangian:

$$\mathcal{L}_{Yukawa} = -\sum_{i,j} Y_{ij}\bar{\psi}_{i,L}\Phi\psi_{j,R} + \text{h.c.} \tag{1.13}$$

.

Once the Higgs field acquires a vacuum expectation value $\langle\Phi\rangle = v/\sqrt{2}$, the fermions gain mass, given by the relation:

$$m_f = Y_f\frac{v}{\sqrt{2}}. \tag{1.14}$$

The masses of fermions vary depending on the value of the Yukawa coupling Y_f. For example, the top quark and bottom quark have very different Yukawa couplings, which explains the significant difference in their masses. Similarly, the electron acquire mass through the same mechanism, though with much smaller Yukawa couplings compared to the heavier quarks.

The differences in Yukawa interactions also determine the flavor mixing structure among quarks (through the Cabibbo-Kobayashi-Maskawa matrix, called CKM matrix) and leptons (through the Pontecorvo-Maki-Nakagawa-Sakata, also called PMNS, matrix), that describe the probability of transitions between different flavours of quarks or leptons, respectively.

1.2 Successes of the Standard Model

The SM of particle physics stands as one of the most successful theoretical frameworks in modern science. It provides a comprehensive description of three of the four fundamental forces (electromagnetic, weak, and strong interactions) and classifies all known elementary particles. Over the past few decades, the SM has been widely tested, and its predictions have been confirmed with remarkable precision in many experiments. In this section, we will discuss the experimental evidence supporting the SM, focusing on major achievements such as the discovery of the neutral currents and of the W and Z bosons, the precision of QED predictions, and the discovery of the Higgs boson.

Discovery of the Weak Neutral Current

One of the earliest and most crucial successes of the Standard Model was the prediction and observation of the weak neutral current. Experiments at CERN provided the first direct evidence for neutral current interactions mediated by the Z^0 boson, a key prediction of the electroweak theory. Before this discovery, only charged currents, mediated by the $W^{\pm}$ bosons, had been observed.

The discovery of neutral currents occurred in 1973 during the Gargamelle experiment, which used a bubble chamber to study neutrino-nucleus interactions [8]. Neutral currents were observed via events where neutrinos interacted with nuclei without producing charged leptons, a phenomenon that was unexpected according to pre-Standard Model theories. In these events, neutrinos scattered exchanging Z^0 bosons and so maintaining their identity (not changing flavor).

The discovery of neutral currents also enabled an early estimation of the Weinberg angle ($\sin^2\theta_W \approx 0.23$), a fundamental parameter that corresponds to the value of the rotation due to the symmetry breaking of the initial plane of vector bosons W^3 and B, producing as a result the Z^0 and the photon. It was determined using Gargamelle's data thanks to the fact that it is related to the ratio of the cross sections in neutral currents and in charged currents. This parameter is essential in the electroweak theory, because it governs the strength of interactions mediated by the W and Z bosons with respect to the photon:

$$gsin\theta_W = g'cos\theta_W = e \tag{1.15}$$

These results were a decisive step toward electroweak unification and cleared the way for the direct discovery of the Z^0 boson and $W^{\pm}$ bosons.

The Discovery of the $W^{\pm}$ and Z^0 Bosons

Another strong evidence to support the SM's electroweak theory was given in 1983, when experiments at the SPS at CERN provided direct evidence for the existence of the $W^{\pm}$ and Z^0 bosons [2]. They were detected in proton-antiproton collisions, where the energy was sufficient to produce these massive particles.

During the experiments events corresponding to the decay of these bosons were observed:

- The W boson was observed through its decay into a lepton and a neutrino ($W \to l\nu$), where the neutrino's presence was inferred from the missing energy.
- The Z boson was detected through its decay into lepton pairs ($Z \to l^+l^-$), such as electron-positron or muon-antimuon pairs.

The Standard Model had predicted the existence and approximate masses of the W and Z bosons based on the weak mixing angle, via the relation:

$$M_W = M_Z cos\theta_W \tag{1.16}$$

The predictions were made using experimental data, for example from neutral current interactions, as explained in the previous section.

- For the W boson, the predicted value of the mass was $M_{W_{th}} \approx 78$ GeV, while the observed one was $M_{W_{exp}} = 81 \pm 2$ GeV (this value was later estimated with further precision measurements to be $M_{W_{exp}} \approx 80$ GeV) [9].
- For the Z boson, the predicted value of the mass was $M_{Z_{th}} \approx 89$ GeV, while the observed one was $M_{Z_{exp}} = 93 \pm 2$ GeV (later measurements have better estimated this value to be $M_{Z_{exp}} \approx 91$ GeV) [9].

This close agreement between the experimental results and the theoretical predictions of the Standard Model was crucial in validating the electroweak theory.

In addition to this, the discovery of the W and Z bosons indirectly provided the first evidence of the spontaneous symmetry breaking mechanism described by the Higgs mechanism, which explains how these bosons acquire mass.

Confirmations of QED and Renormalizability

In computations of particle interactions, when considering quantum corrections (loops), it can happen to get divergences, but the SM's renormalizability guarantees that these divergences can be reabsorbed in the fundamentals parameters (such as masses and charges), so that it is still possibile to get precise predictions that can be tested experimentally.

The verification of renormalizability in QED [1] has been made possible through highly precise measurements of physical quantities, such as the anomalous magnetic moment of the electron (g_e) and the properties of the W and Z bosons, performed at CERN's LEP.

Discovery of the Higgs Boson

The crowning achievement of the Standard Model came in 2012 with the discovery of the Higgs boson at CERN's LHC. The Higgs boson is the quantum manifestation of the Higgs field, which is responsible for the spontaneous breaking of the electroweak symmetry and the generation of mass for the W and Z bosons, as well as for fermions through the Yukawa interactions.

The Higgs boson was the last missing piece of the Standard Model, and its discovery provided crucial experimental confirmation of the Higgs mechanism. The mass of the Higgs boson, measured at approximately 125 GeV, was consistent with the constraints provided by previous experiments, such as those at LEP and the Tevatron, which had ruled out large portions of the Higgs mass range.

1.3 Limitations of the Standard Model

While the Standard Model has been successful in explaining a wide variety of particle physics phenomena, it is incomplete as a theory of fundamental interactions. It fails to address several important questions and cosmological observations, suggesting the existence of new physics beyond the Standard Model. In this section, we will provide a glimpse of some limitations of the Standard Model, including issues related to baryogenesis, dark matter, the strong CP problem, the gauge hierarchy problem, neutrino masses, grand unification, and dark energy.

Baryogenesis

The universe exhibits a clear matter-antimatter asymmetry, with an excess of matter over antimatter. The baryon-to-photon ratio, which has been measured with high precision and is of order $n_b/n_\gamma \approx 10^{-10}$, suggests that there has been a mechanism in place during the early universe that has favored the production of baryons over antibaryons, allowing for baryogenesis.

According to the Sakharov conditions, generating this asymmetry requires baryon number violation, CP violation, and a departure from thermal equilibrium. Although the Standard Model contains sources of CP violation in weak interactions, they are insufficient to account for the observed baryon asymmetry. New physics beyond the SM is required, and proposed mechanisms often involve additional CP-violating interactions or new particles that could explain baryogenesis. Chapter 2 will explore the Baryogenesis topic in more depth.

Dark Matter

Astrophysical and cosmological observations have provided compelling evidence for the existence of DM, which accounts for approximately 27% of the universe's energy density. Evidence for dark matter comes from galaxy rotation curves, gravitational lensing, the cosmic microwave background, and the LSS of the universe. However, the Standard Model does not include any suitable candidates for dark matter. Neutrinos, the only SM particles that interact weakly, are too light and would constitute "hot dark matter", which behavior could not explain the observed structure formation.

This discrepancy has led to the proposal of introducing a new kind of stable and weakly interacting particles, often referred to as WIMPs (see section 3.2), and other exotic candidates such as axions. The dark matter issue will be discussed in more detail in chapter 3.

Strong CP problem

QCD, the theory of the strong interaction, allows for a CP-violating term in its Lagrangian, parameterized by the angle θ_{QCD}. If θ_{QCD} was of order one, it would induce a large electric dipole moment for the neutron, which has not been observed experimentally. Instead, experimental observations indicate that θ_{QCD} must be less than 10^{-10}, raising the question of why this parameter is so small. The reason for this smallness is unexplained within the SM, and this is known as the strong CP problem.

One possible solution is the Peccei-Quinn mechanism [12], which introduces a new global symmetry that dynamically drives θ_{QCD} to zero. This mechanism predicts the existence of a new particle, called axion, which we already mentioned as it is also a potential dark matter candidate.

Grand Unification Theories

Grand Unification Theories (GUT) aim to unify the three fundamental interactions, described by the SM using three distinct gauge groups:

$$SU(3)_C \times SU(2)_L \times U(1)_Y,$$

into a single, larger symmetry group, such as SU(5). These would merge at extremely high energies ($E_{GUT} \approx 10^{15} - 10^{16}$): as the universe cooled after the Big Bang, this unified symmetry would have spontaneously broken into the three separate forces observed today. In the SM, the coupling constants of the the three forces vary with energy, and these theories predict that they should converge at the GUT scale. Experimental measurements indicate that within the SM this unification does not occur, while other theories (like Supersymmetry) predict it, but to this day there is no experimental evidence for their predictions.

Neutrino Masses

In the Standard Model neutrinos are assumed to be massless, since it is not expected to exist a neutrino right ν_R. However, the discovery of neutrino oscillations (propagating neutrinos can change flavor) have proved that neutrinos have small but non-zero masses: this fact indicates the need of some new physics beyond the SM, to include a mechanism that gives mass to neutrinos.

One widely studied solution is the so-called "seesaw mechanism", which introduces heavy right-handed neutrinos (too heavy to be produced at our energies). A possibility for this new physics energy scale could be the same of GUT scale, so this constitutes an important area of research in both theoretical and experimental physics .

The Gauge Hierarchy problem

The gauge hierarchy problem concerns the large disparity between the electroweak scale, where the Higgs boson mass is observed (around 125 GeV), and the Planck scale ($\sim 10^{19}$ GeV), at which gravitational interactions become significant. In computing the Higgs boson mass, contributions in the loops of superheavy virtual GUT particles should be taken into account, driving it to values near the Planck scale.

One solution to this problem could be an extreme fine-tuning of parameters in order to cancel these corrections, but this is considered unnatural, thus other theories to extend the SM are needed (for example some proposals include Supersymmetry and extra-dimensions theories).

Dark Energy and Cosmological Implications

DE is defined as a form of energy that permeates the space and exerts a negative pressure, that is counteracting the attractive force of gravity, driving the accelerated expansion of the universe. It accounts for about 68% of the universe's energy density. The Standard Model does not provide any explanation for the origin or nature of dark energy, as it doesn't include gravity and the accelerated universe's expansion in the phenomenons that are explained in the theory.

The cosmological constant, Λ, is currently the simplest possible solution: it is a term added to Einstein's equations that acts as a repulsive force, causing space to expand. However this term raises the question of why it has such a small value compared to theoretical predictions, again a fine-tuning problem.

1.4 Conclusion

In this first chapter, we have presented an overview of the Standard Model of particle physics, its theoretical foundations, experimental successes, and its intrinsic limitations. The Standard Model, despite its strong predictive power and its experimental validation - presented in Section 1.2 - is not a complete theory of fundamental interactions.

The list of issues discussed in Section 1.3, although comprehensive, has necessarily been treated at an introductory and non-exhaustive level. Each of the mentioned problems, such as the gauge hierarchy problem, the origin of neutrino masses, the strong CP problem, the research of a dark matter candidate, and the mechanisms behind the observed baryon asymmetry, opens up wide research fields, each deserving dedicated and extensive discussions. The aim of this chapter, however, was not to provide a complete treatment of each issue, but rather to outline the broader landscape of open questions that motivate the search for physics beyond the Standard Model.

In particular, in the continuation of this work, we will cover in more detail two aspects among those mentioned in this section: the matter-antimatter asymmetry of the Universe (baryogenesis) and the nature of dark matter. These two phenomena not only require new theoretical frameworks but may also share common origins, suggesting the existence of unified solutions that address multiple open problems simultaneously.

The next chapters will thus explore baryogenesis mechanisms, dark matter, and the possibility of a common explanation, setting the stage for the detailed analysis of the WIMPy baryogenesis scenario.

2

Baryogenesis

The observed dominance of matter over antimatter in the Universe is one of the most fundamental issues in modern cosmology. It is a critical condition for the existence of stars, galaxies, and ultimately life as we know it. However the Standard Model of particle physics, while containing the seeds of some necessary ingredients, does fail in quantitatively explaining the observed baryon asymmetry.

In this chapter we will explore the theme of matter-antimatter asymmetry and baryogenesis (the class of theoretical mechanisms that attempt to dynamically generate a net baryon number from an initially symmetric state in the early Universe). In Section 2.1 we will briefly present the observational evidences that support the asymmetry and we will give an overview of the problem; in Section 2.2 we will present the characteristics that a model should satisfy in order to solve it. In particular, we will list the theoretical conditions required to generate such an asymmetry and examine their implementation within the Standard Model framework. Finally we will introduce a simplified toy model that displays the essential features of a baryogenesis process.

2.1 Matter-Antimatter Asymmetry

2.1.1 Observational Evidence

On Earth and in the solar system antimatter is found only in extremely small quantities (excluding its presence in high-energy physics experiments).

Indeed, planetary probes have confirmed that planets in the solar system are composed of matter, as shown by the lack of catastrophic matter-antimatter annihilations. Cosmic rays, that provide material from further regions, show presence of antiprotons at order 10^{-4} with respect to the number of protons, a quantity that suggests secondary production from cosmic ray collisions rather than primordial antimatter. In addition to that, searches for heavier antimatter, as anti-He^4, have yielded no conclusive detections.

On larger scales, there would be strong γ-ray emission due to nucleon-antinucleon annhiliations if there existed both matter galaxies and antimatter galaxies inside a single cluster (since clusters contain intracluster gas), and this has never been detected.

To quantify this asymmetry we use the Baryon number, defined as:

$$B = \frac{n_B}{s} \tag{2.1}$$

where s is the entropy density and n_B the net baryon number density, $n_B = n_b - n_{\bar{b}}$. This number corresponds to the net baryon number in a comoving volume and is conserved in absence of baryon number violating reactions and entropy injections in the Universe (see appendix A for more details). Another parameter that well represents the situation is the baryon-to-photon ratio:

$$\eta = \frac{n_B}{n_\gamma} = 1.8 g_{*s} B \tag{2.2}$$

where for the second equation it has been used the relation $s = 1.8 g_{*s} n_\gamma$.

The two key measurements of the asymmetry are provided by:

- The CMB, a remnant radiation from the early universe, that carries information about the baryon density at that time through fluctuations in its temperature and polarization.

- The BBN, the process of formation of light nuclei in primordial universe. The abundance of these elements critically depends on the baryon-to-photon ratio η, which determines the density of baryons available to participate in nuclear reactions.

Experimental data from CMB and BBN, separately, allow to infer a value for the baryon-to-photon ratio of order [5]:

$$\eta \approx 6 \cdot 10^{-10}. \tag{2.3}$$

This agreement between CMB and BBN measurements is an important success of modern cosmology, strongly supporting the existence of a small but nonzero baryon asymmetry.

2.1.2 Implications for the Matter-Antimatter Asymmetry

We can analyze some of the simplest initial conditions regarding the abundances of baryons and antibaryons in the early universe:

- The most logical initial condition would be to have $n_b = n_{\bar{b}}$, in this case baryons and antibaryons would annihilate until the end of chemical equilibrium (as their number decreases it becomes more difficult to find couples $b - \bar{b}$). That would happen at a temperature T ≈ 22 MeV, when $\frac{n_b}{s} = \frac{\bar{b}}{s} \approx 10^{-20}$, meaning that starting from a symmetric universe in matter-antimatter today we should have much less matter than the observed value.

- We could assume that, as an initial condition, only matter was present, and that antimatter was subsequently produced through collisions in the primordial plasma. In such a scenario, we would expect that, as in the early Universe, $x_B = x_\gamma$ even today. However, the measured value of η indicates that matter is extremely rare compared to photons - a fact that requires an explanation.

- Another option could be that in early universe there were both baryons and antibaryons, with a slight imbalance in favor of the first. In this scenario starting from a large number of quarks and anti-quarks, $n_q \approx n_{\bar{q}} \approx n_\gamma$, after all the annihilations it would remain only the small fraction of baryons that we observe today. However, the initial asymmetry needed to obtain the present result is so small that this pathway seems quite unlikely.

For these reasons, baryogenesis is presented as a scenario worthy of interest, since it searches ways to dynamically obtain an asymmetry in a Universe that is initially baryon symmetric, or even regardless of any symmetry or asymmetry in the initial conditions.

2.2 Baryogenesis model

2.2.1 Sakharov conditions

In order to generate a baryon asymmetry from an initially symmetric universe there are three condition needed, called Sakharov conditions from the physicist that formulated them in the 1960s:

- Baryon number violation: there must exist some interactions that do not conserve B in order to create an asymmetry. If B was strictly conserved in every interaction, a universe initially symmetric would remain such.

- C (charge conjugation) and CP (charge conjugation combined with parity) violation: a preference for matter over antimatter (or viceversa) is needed to produce them with different rates in B-violating interactions, generating a nonzero net baryon number. Without CP violation, the rate of baryon-producing processes would be the same as the rate of the complementary processes producing antibaryons.

  The need for these two conditions can be analyzed more in detail:

  1. C violation: charge conjugation symmetry transforms particles into their corresponding antiparticles, so, if this symmetry was respected, to each process that produces baryons it would correspond an equally probable counterpart producing antibaryons:

     $$\Gamma(X \rightarrow B) = \Gamma(\bar{X} \rightarrow \bar{B}), \tag{2.4}$$

     where X is a generic particle decaying into baryons (B), and $\bar{X}$, $\bar{B}$ the charge conjugated particles. Thus, no net baryon number B would be generated.

  2. CP violation: C violation alone is not sufficient, and we can prove this by thinking of a generic particle X that is subject to decays:

     $$X \rightarrow q_L q_L, \qquad X \rightarrow q_R q_R, \tag{2.5}$$

     with q_L and q_R representing respectively left-handed and righ-handed quarks, that transform under CP as $q_{L(R)} \rightarrow \bar{q}_{R(L)}$. If CP was an exact symmetry, it would follow that:

$$\Gamma(X \to q_L q_L) = \Gamma(\bar{X} \to \bar{q}_R \bar{q}_R), \qquad \Gamma(X \to q_R q_R) = \Gamma(\bar{X} \to \bar{q}_L \bar{q}_L), \tag{2.6}$$

which results:

$$\Gamma(X \to q_L q_L) + \Gamma(X \to q_R q_R) = \Gamma(\bar{X} \to \bar{q}_R \bar{q}_R) + \Gamma(\bar{X} \to \bar{q}_L \bar{q}_L) \tag{2.7}$$

that means there is no asymmetry created.

From this reasoning we can conclude that both C and CP symmetries must be non conserved to obtain a net baryon number.

- Out of equilibrium condition: an intuitive explanation can be given thinking to the example of decay that has been considered above, a generic particle X that decaying produces a baryon B. Thermal equilibrium would imply that the inverse process has the same rate:

$$\Gamma(X \to B) = \Gamma(B \to X), \tag{2.8}$$

obtaining no net baryon asymmetry since B is destroyed by the inverse process as fast as it is produced.

This question can also be presented in terms of the number densities. The thermal equilibrium condition implies that the chemical potentials of baryons and antibaryons, corresponding to μ_b and $\mu_{\bar{b}}$, are equal to zero. In addition to this, CPT invariance guarantees the equality of the masses and of the energies, since $E = \sqrt{p^2 + m^2}$. With this condition, the phase space distribution function

$$f = \frac{1}{e^{\frac{E-\mu}{T}} \pm 1} \tag{2.9}$$

is the same for baryons and antibaryons. It follows that not imposing the out of equilibrium condition it would result that $n_b = n_{\bar{b}}$, which means B = 0.

In the next subsection we will consider these conditions and their viability in the Standard Model framework.

2.2.2 Sakharov Conditions in the Standard Model and Electroweak Baryogenesis

In the Standard Model are present all the necessary ingredients to investigate whether the Sakharov conditions can be satisfied within its framework. In particular:

- Baryon number can be violated if we take into account nonperturbative processes (spharelons);
- C is maximally violated within the SM by Weak Interactions (the currents involve only left handed fields), while CP is violated in the Electroweak sector thanks to the presence of a complex phase in the V_{CKM} matrix;
- During the Electroweak symmetry breaking there could be, in principle, the conditions for a deviation from equilibrium and the production of a net Baryon number B.

However, as will be briefly shown here, these effects are not efficient enough to provide the observed baryon asymmetry.

Baryon Number Violation in the Standard Model

While baryon (B) and lepton (L) numbers are conserved in the SM at tree level and perturbative level, they are violated by nonperturbative electroweak processes called sphalerons. Sphalerons are static, saddle point solution to the field equations. These processes consist in transitions between different vacuum states of the electroweak theory that violate B and L numbers, but preserve the difference $B-L$. They can happen at high temperatures ($T \geq 100$ GeV), at which they are no longer exponentially suppressed since there is no tunneling.

Since sphaleron transitions are active in the symmetric phase, any generated baryon asymmetry can be erased if these processes remain in thermal equilibrium [5].

CP Violation in the Standard Model

CP violation in the SM arises from the complex phase δ in the Cabibbo-Kobayashi-Maskawa (CKM) matrix, that describes flavor mixing of quarks in weak interactions:

$$V = \begin{bmatrix} V_{ud} & V_{us} & V_{ub} \\ V_{cd} & V_{cs} & V_{cb} \\ V_{td} & V_{ts} & V_{tb} \end{bmatrix}.$$

The amount of CP violation is parameterized by an invariant that results in a suppression factor in the final value of B. This suppression factor, δ_{CP}, is of order $\sim 10^{-20}$, providing a baryon asymmetry several orders of magnitude below the observed value [13]. Therefore, the SM does not provide sufficient CP violation for successful baryogenesis.

Electroweak Phase Transition and Electroweak Baryogenesis

Electroweak baryogenesis (EWBG) is a theory that proposes the origin of the observed baryon asymmetry of the Universe taking place during the electroweak phase transition (EWPT). In order to obtain a successful baryogenesis, it is required that the phase transition is of first order, meaning it proceeds via bubble nucleation.

Specifically, the mechanism proceeds this way: at high temperatures the Higgs field vacuum expectation value (VEV) $\langle\phi\rangle$ is zero (we are in the symmetric phase); then, with the universe cooling down, a second local minimum forms, separated by an energy barrier. As the temperature decreases and goes under a critical value T_c - the value at which the two vacua are energetically equivalent - there are bubbles of the broken phase, where is has taken place the phase transition and the Higgs field acquired a VEV $\langle\phi\rangle \neq 0$, that nucleate and expand.

As these bubbles expand in the symmetric phase, they create local thermal non-equilibrium at the moving bubbles walls, satisfying the third Sakharov condition for baryogenesis.

Because of CP-violating interactions in the bubble walls, a CP-asymmetry accumulates on the two sides of the walls. In the unbroken phase side, where it happen sphaleron processes that violate baryon number, the CP asymmetry gets converted into a baryon asymmetry, while inside the broken phase sphaleron processes are supposed to be suppressed. The baryons formed, due to the expansion of the walls, can diffuse inside the bubbles, that eventually will merge and fill the universe.

In order for the produced baryon asymmetry to remain, leading to the condition observed today, the requirement is the suppression of B violating sphaleron transitions inside the bubbles, meaning the Higgs VEV must satisfy:

$$\frac{\langle \phi(T_c) \rangle}{T_c} \gtrsim 1,$$

that corresponds to a strongly first-order transition.

However, it has been shown that this condition is not met in the Standard Model: infact, for Higgs masses $m_H > 80$GeV, the phase transition is not a first order one, instead it is second order (which is rather a smooth crossover): the sphalerons pass from equilibrium to out of equilibrium in a continuous and uniform in space way, not allowing to the bubble nucleation scenario.

The difference between a first order and second order phase transition can be seen in figure 2.1, which displays the evolution of the Higgs potential at varying T.

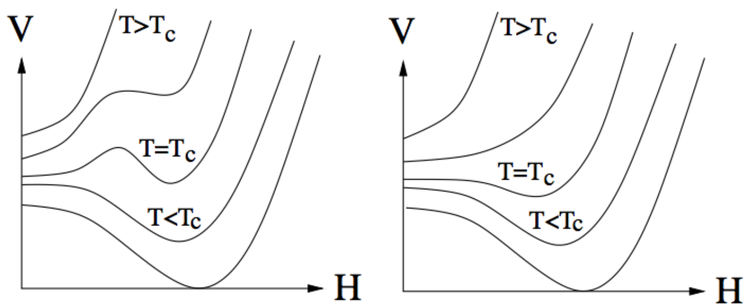

Figure 2.1: Left picture: schematic illustration of Higgs potential for different temperatures for first order phase transition; Right picture: schematic illustration of Higgs potential for different temperatures for second order phase transition [4].

In conclusion, the electroweak baryogenesis would be an attractive mechanism since it relies on physics testable at the electroweak scale. However, taken together, these limitations suggest that the Standard Model cannot simultaneously satisfy all three Sakharov criteria at a level sufficient to explain the observed asymmetry, and this provides a strong motivation for the search and development of new physics beyond the Standard Model.

2.2.3 Toy model

We will now present a toy model for Baryogenesis that relies on out of equilibrium decays.

We assume that there is a particle X, massive and with zero baryon number, that decays into two channels:

- $X \longrightarrow qq$, with a final state baryon number B = $\frac{2}{3}$ and branching ratio $\frac{\Gamma_{X\to qq}}{\Gamma_{TOT}} = r$.
- $X \longrightarrow \bar{q}\bar{l}$, with a final state baryon number B = $-\frac{1}{3}$ and branching ratio $\frac{\Gamma_{X\to \bar{q}\bar{l}}}{\Gamma_{TOT}} = 1 - r$.

For the antiparticle $\bar{X}$, instead, the decay channels are:

- $\bar{X} \longrightarrow \bar{q}\bar{q}$, with a final state baryon number B = $-\frac{2}{3}$ and branching ratio $\frac{\Gamma_{\bar{X}\to \bar{q}\bar{q}}}{\Gamma_{TOT}} = \bar{r}$
- $\bar{X} \longrightarrow ql$, with a final state baryon number B = $\frac{1}{3}$ and branching ratio $\frac{\Gamma_{\bar{X}\to ql}}{\Gamma_{TOT}} = 1 - \bar{r}$.

The mean net baryon number produced by the decay of X and $\bar{X}$, that we will name ϵ, is the sum of the baryon numbers produced by each particle decays:

$$B_X = \frac{2}{3}r - \frac{1}{3}(1 - r) = r - \frac{1}{3} \tag{2.10}$$

$$B_{\bar{X}} = -\frac{2}{3}\bar{r} + \frac{1}{3}(1 - \bar{r}) = -\bar{r} + \frac{1}{3} \tag{2.11}$$

$$\epsilon = B_X + B_{\bar{X}} = r - \bar{r} \tag{2.12}$$

It follows that in order to have generation of a mean net baryon number different from zero, r should differ from $\bar{r}$ (which means C and CP are not conseved).

The amount of violation needed can be estimated knowing the measured value of B:

$$B = \frac{n_B}{s} \approx \frac{\epsilon n_X}{1.8 g*_s\, n_\gamma} \approx \frac{\epsilon n_\gamma}{1.8 g*_s\, n_\gamma} \approx \frac{\epsilon}{g*_s} \approx 10^{-10} \tag{2.13}$$

where all terms are considered at the decay time, and assuming that in the early Universe the initial abundance of X, $\bar{X}$ bosons is thermal ($n_X = n_{\bar{X}} \approx n_\gamma$). We can deduce that ϵ should be of order $10^{-8\div7}$, a small value indeed.

Actually it should be noted that at tree level $\Gamma(X \longrightarrow qq)$ and $\Gamma(\bar{X} \longrightarrow \bar{q}\bar{q})$ are equal, so we should take into account also higher orders: a contribution to ϵ can be found in the interference of the tree level diagram with the loop level one. See [10] for more details.

We can now analyze the out of equilibrium decay scenario. During Universe's expansion, if the interactions rate (Γ) of particles X, $\bar{X}$ is slower than the expansion rate (H), it occurs a departure from equilibrium. In an equilibrium scenario we would have:

- $n_X = n_{\bar{X}} \approx n_\gamma$ when X particles are relativistic (T>m_X), as we assumed previously
- $n_X = n_{\bar{X}} \approx (m_X T)^{3/2} e^{-m_X/T} << n_\gamma$ when X are nonrelativistic (T<m_X).

The principal interaction modes for X are their decays and inverse decays, scattering processes mediated by X, and annihilations, that can be neglected since they're important at the beginning but quickly suppressed ($\Gamma_{ann} \propto n_X$). The rates for these interactions are:

$$\Gamma_D \simeq \alpha m_X \begin{cases} m_X/T & T > m_X \\ 1 & T < m_X \end{cases} \tag{2.14}$$

$$\Gamma_{ID} \simeq \Gamma_D \begin{cases} 1 & T > m_X \\ (m_X/T)^{3/2} e^{-m_X/T} & T < m_X \end{cases} \tag{2.15}$$

$$\begin{aligned} &\Gamma_S \simeq n\sigma \simeq T^3 \alpha \frac{T^2}{(T^2 + m_X^2)^2}, \\ &\begin{cases} \sigma \simeq \dfrac{\alpha^2}{T^2} & T >> m_X \\ \sigma \simeq \dfrac{\alpha^2 T^2}{m_X^4} \simeq G_X^2 T^2 & T << m_X \end{cases} \end{aligned} \tag{2.16}$$

In order to study this scenario, it is now helpful to introduce a quantity that compares the decay rate with the expansion rate $H = g*^{1/2}\, T^2/M_{PL}$ at $T = m_X$:

$$K \equiv \left(\frac{\Gamma_D}{H}\right)\bigg|_{T=m_X} \approx \frac{\alpha M_{PL}}{g*^{1/2}\, m_X}. \tag{2.17}$$

This formula measures the efficiency of the decays when the particle X starts to be nonrelativistic.

It is easy to verify that decays are the most important process in the baryogenesis scenario:

$$\frac{\Gamma_{ID}}{H}\bigg|_{T\leq m_X} \approx K e^{-m_X/T} \tag{2.18}$$

$$\frac{\Gamma_S}{H}\bigg|_{T\leq m_X} \approx \alpha K \left(\frac{T}{m_X}\right)^3 \tag{2.19}$$

both ratios are suppressed with respect to K.

If we impose the condition K « 1, we would obtain X at $T = m_X$ to be already out of equilibrium, which means that they decouple being relativistic. In this case, after the exit from equilibrium, the quantity of X and $\bar{X}$ do not decrease and an overabundance is produced with respect to the equilibrium scenario. Then, since $H \sim T^2$, at some point Γ_D will be larger than H for sure, so these particles will just decay, with no inverse process (see fig. 2.2).

Having assumed that each decay produces a mean net baryon number ϵ, this mechanism would provide nonzero Baryon asymmetry, as desired.

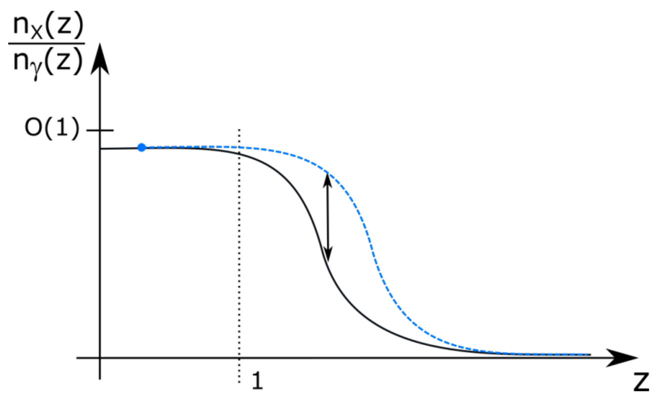

Figure 2.2: The solid line represents the equilibrium distribution behavior n_X^{eq}/n_γ as function of $z = m_X/T$, while the dashed line represents the expected real ratio n_X/n_γ, if the X decouples while being relativistic. The overabundance is the difference between the two lines, highlighted by the arrow[7].

The condition K « 1 results in a restriction for the X boson mass:

$$m_X >> \frac{\alpha M_{PL}}{g^{*1/2}} \sim \frac{\alpha}{10^{-2}} 10^{16} GeV \tag{2.20}$$

that can be observed, taking for example the magnitude of α for gauge bosons $\alpha \sim 10^{-2}$, entails a very large value for m_X.

In the opposite condition, K » 1, we would expect the number density n_X to follow the equilibrium value (solid line in fig. 2.2), not producing a baryon asymmetry. If instead we want to consider the intermediate case, $K \sim 1$, we would need to follow the Boltzmann equations in detail, as presented in the Appendix B.

2.3 Conclusion

In this chapter we have seen that the existence of a non-zero baryon-to-photon ratio is a well-established fact, supported by precise measurements from the Cosmic Microwave Background and Big Bang Nucleosynthesis.

To explain this asymmetry dynamically, we presented the Sakharov conditions that a model must satisfy to be viable: baryon number violation, C and CP violation, and departure from thermal equilibrium. Although the Standard Model contains ingredients pointing in the right direction, the effects are quantitatively insufficient: in particular, the electroweak phase transition is not strongly first-order for the observed Higgs mass, preventing the required out-of-equilibrium conditions for electroweak baryogenesis.

To illustrate the basics of baryogenesis in a simplified setting, we introduced a toy model where CP-violating decays of a heavy particle can generate a net baryon number. This model highlights the role of out of equilibrium decays and provides an intuitive description of a small asymmetry dynamical generation in the early Universe.

These considerations suggest that new physics beyond the Standard Model is needed to account for the baryon asymmetry. In the following chapter, as we hinted previously, we will explore another significant unresolved issue in cosmology the nature of dark matter to then investigate a common origin of dark matter and baryogenesis in the continuation.

3

Dark Matter

The nature of dark matter remains one of the most fascinating unresolved questions in modern physics and cosmology. Although dark matter does not interact significantly with electromagnetic radiation, and is thus invisible to conventional telescopic observations, its gravitational effects are well evident. Dark matter's influence manifests across various scales, from the dynamics of individual galaxies to the formation of large scale structures, which makes it an essential actor in the shaping of Universe.

In this chapter we start in Section 3.1 by presenting and discussing the main observational evidences that support the existence of dark matter; then, in Section 3.2 we focus on one of the most promising dark matter candidates: Weakly Interacting Massive Particles (WIMPs). In this section we also introduce the Boltzmann equation framework used to describe the number density evolution of WIMPs over time.

3.1 Evidences for Dark Matter

The existence of a particular kind of matter that interacts through gravity but doesn't emit, or absorb or reflect electromagnetic radiation, and for this reason has earned the appellation of "dark", has been made evident by many astrophysical observations. These observations regard different scales, from a single galaxy's scale to the scale of LSS of the universe.

3.1.1 Galactic Scale Evidence

One of the most direct evidences for dark matter comes from the study of galactic rotation curves: in spiral galaxies, the observed rotational velocities of stars and gas remain approximately constant at large distances from the galactic center. This behavior doesn't match the expectation based on visible matter alone, since the circular velocity is expected to be $v(r) = \sqrt{\frac{GM(r)}{r}}$, with $M(r) = 4\pi \int \rho(r) r^2 dr$ and the mass density profile $\rho(r) \propto 1/\sqrt{r}$ (decreasing beyond the optical disk). These observations are helped by the presence of LSB galaxies, where the contribution from visible matter is very low and the dynamics are thought to be almost entirely dominated by dark matter. In conclusion, from rotation curves of both low and high surface luminosity galaxies it can be inferred a density profile that is quite general, composed by the visible stellar disk and a spherical halo of invisible matter enveloping galaxies (with some uncertainties about the flatness of the core) [3].

3.1.2 Evidence from Galaxy Clusters

At larger scales, galaxy clusters provide other evidences for dark matter existence. The first hints came from Fritz Zwicky' s studies on the Coma Cluster in the 1930s, who, by measuring the velocities of galaxies, deduced a mass-to-light ratio two orders of magnitude larger than the one characteristic of the solar system, suggesting the presence of a large amount of non-visible mass [14].

Many modern studies have confirmed this finding, among them can be listed [3]:

- Estimates from gravitational lensing effect: light's geodesics are deflected by strong gravitational fields, so observing distant galaxies it can be mapped the presence of dark matter by the distortion of light.
- X-rays emissions: observations of hot intracluster gas distribution reveal that the total gravitational mass is significantly greater than the visible baryonic mass.
- Hydrostatic studies: from the hydrostatic equilibrium equation, using the density profile of the observed gas, it can be derived an expected temperature for the clusters that is much lower than the measured temperature, which suggests the existence of a large amount of dark matter.

3.1.3 Cosmological scale evidence

On cosmological scales, the study of the cosmic microwave background has been of crucial importance for the confirmation of DM existence and for the estimation of its total amount, as well as the amount of the other elements constituting the Universe.

CMB is a cosmic radiation coming from photons that decoupled in the early universe, it presents a black body spectrum with a temperature T = 2.726 K and it is almost isotropic. It presents however some small anisotropies, that are of fundamental importance to us since from them it is possible to extract information about the cosmological parameters.

In particular, WMAP data has revealed values for the abundance of baryons in the Universe of order $\Omega_b h^2 \sim 0.02$, while for the total amount of matter $\Omega_M h^2 \sim 0.14$ [3].

3.1.4 Numerical simulations

N-body simulations have played a critical role in understanding the role of dark matter in large-scale structure formation. These simulations well replicate the observed distribution of galaxies and clusters when dark matter is included, and indicate that dark matter follows a universal profile with hierarchical structures, shaping the universe as we observe it today. Different studies have shown different results for the density profile behavior in the innermost regions of galaxies and galaxy clusters, but its overall shape, with the slope increasing moving from the center to the outer regions, is clear from all the simulations [3].

3.2 WIMPs as Dark Matter Candidates

The research for dark matter candidates is concentrated in finding new kind of particles that are stable and neutral.

Neutrinos are the only particles in SM that satisfy these conditions, but they cannot account for dark matter for two main reasons: firstly, considering the tightest upper bound on the neutrinos masses $\sum_i m_\nu^i \lesssim 0.12$eV, they would provide $\Omega_\nu \lesssim 10^{-3} << \Omega_{DM} \sim 0.27$ [7]; secondly, neutrinos are still relativistic when they decouple - meaning they would constitute a hot kind of dark matter - so their large velocity dispersion would be expected to stop the growth of seeds of matter, countering density anisotropies on small scales. This would lead to a different LSS formation process and in the end to a different matter structure of the Universe.

For the reasons just mentioned, the majority of the researches for possible dark matter particles focus on the category of cold dark matter, which is already non-relativistic when it decouples.

WIMPs are among the most studied theoretical candidates for DM. These hypothetical particles emerge from the ensemble of candidates because they are naturally present in extensions to the SM of particle physics and they can explain the observed relic abundance of DM in the universe through the thermal freeze-out mechanism. In the following, we will give an idea of the theoretical foundations of WIMPs and the reasons for their success.

The theoretical origin of these particles must be sought in supersymmetric theories, and in the research for new physics close to the electroweak scale that solves the gauge hierarchy problem. In fact, WIMPs are typically expected to have masses of the order $O(100GeV)$ and to interact through weak-scale forces, as their name suggests.

Initially, they were in thermal equilibrium with the other SM particles via annihilation and creation processes, then, with Universe expanding, their interaction rate became lower than the expansion rate and they decoupled from the plasma, leaving a relic abundance of WIMPs. The only process responsible for the decrease in the population of WIMPs is annihilation, since we're considering them to be stable particles, so the freeze-out condition is:

$$\Gamma_X^{ann} = H. \tag{3.1}$$

The evolution of the WIMPs abundance in the early universe is governed by the Boltzmann equations (see appendix B), and below it will be analyzed more in detail.

3.2.1 Boltzmann equations for WIMPs

We consider a generic particle Ψ that is subject to annihilation into SM particles X:

$$\Psi\bar{\Psi} \longleftrightarrow X\bar{X} \tag{3.2}$$

where X are in thermal equilibrium with the plasma, and $n_\Psi = n_{\bar{\Psi}}$, $n_X = n_{\bar{X}}$. Exploiting what is developed in the appendix B, for the case of Ψ, we can write the following equation for the evolution of n_Ψ:

$$\dot{n}_\Psi + 3Hn_\Psi = -\langle\sigma|v|\rangle(n_\Psi^2 - n_\Psi^{2eq}). \tag{3.3}$$

We can now use the time variable $x = m_\Psi/T$ and define the abundance of Ψ particles $Y \equiv n_\Psi/s$, obtaining:

$$a^{-3}(\dot{a^3 n_\Psi}) = s\dot{Y} = -\langle\sigma|v|\rangle(n_\Psi^2 - n_\Psi^{2eq}) \tag{3.4}$$

$$\frac{dY}{dx} = -\frac{\langle\sigma|v|\rangle}{xH}s(Y^2 - Y_{eq}^2) \tag{3.5}$$

$$\frac{dY}{dx} = -\frac{\langle\sigma|v|\rangle}{H(x=1)}xs(Y^2 - Y_{eq}^2). \tag{3.6}$$

The terms of the equation with + and - sign represent, respectively, the annihilations of Ψ particles (their decrease in number), and the term at equilibrium, at which X particles are energetic enough to form back Ψ.

Y_{eq} corresponds to:

$$Y_{eq}(x) \approx \begin{cases} \dfrac{g_{eff}}{g*_s} & x << 1 \\ 0.145\dfrac{g_\Psi}{g*_s}x^{3/2}e^{-x} & x >> 1, \end{cases} \tag{3.7}$$

with g_Ψ the internal DOF of Ψ, and

$$g_{eff} = \begin{cases} g_\Psi & \text{for bosons} \\ \dfrac{3}{4}g_\Psi & \text{for fermions.} \end{cases} \tag{3.8}$$

Equation 3.6 can be further simplified by writing it in the form:

$$\frac{x}{Y_{eq}}\frac{dY}{dx} = -\frac{\langle\sigma|v|\rangle n_\Psi^{eq}}{H}\left[\left(\frac{Y}{Y_{eq}}\right)^2 - 1\right] = -\frac{\Gamma_{ann}}{H}\left[\left(\frac{Y}{Y_{eq}}\right)^2 - 1\right] \tag{3.9}$$

so that we have the ratio Γ_{ann}/H, that represents the efficiency of the annihilation processes: when Γ_{ann}/H « 1 the relative variation of Y, $\Delta Y/Y \sim \Gamma_{ann}/H$, is $<< 1$. The equilibrium value n_Ψ^{eq}, in fact, is suppressed as $\sim e^{-x}$ for $x >> 1$. The resulting situation is that until the freeze-out epoch, the abundance of Ψ will follow the equilibrium distribution:

$$Y(x) \approx Y_{eq}(x) \qquad x \leq x_f, \tag{3.10}$$

while after the freeze-out, the number of Ψ particles in a comoving volume will remain constant:

$$Y_{eq}(x) << Y(x) \approx Y_{eq}(x_f) \qquad x >> x_f. \tag{3.11}$$

Since we are considering WIMPs, that are a kind of cold DM[1], they will follow the equilibrium curve partially also in the suppressed region, so the moment of the decoupling is crucial for the final abundance because a small difference corresponds to a large gap in the result (see fig. 3.1).

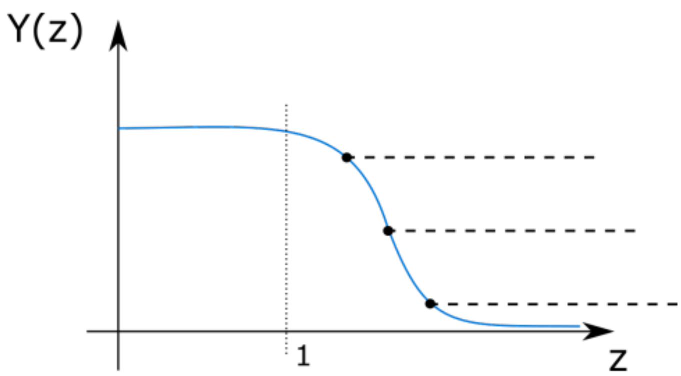

Figure 3.1: The solid line is the Boltzmann suppressed equilibrium behavior; the dashed lines, instead, are the expected behavior of WIMPs particles for different moments of decoupling at $z = m_X/T > 1$. It is possible to appreciate from this illustration the sensible role that the decoupling moment plays in the final abundance generation[7].

Here, we can write $\langle\sigma|v|\rangle = \sigma_0\left(\frac{T}{m_\Psi}\right)^n = \sigma_0 x^{-n}$, and eq. (3.6) can be recast as:

$$\frac{dY}{dx} = -\frac{\lambda}{x^{n+2}}(Y^2 - Y_{eq}^2), \tag{3.12}$$

[1] i.e. decoupling when nonrelativistic.

where

$$\lambda \equiv \frac{x^3\sigma_0 s}{H(x=1)} \simeq \frac{m_\Psi^3\sigma_0 T^3 g*_s}{T^3 g*^{1/2}(x=1)m_\Psi^2/M_P} \approx 0.264 M_P m_\Psi \sigma_0 \frac{g*_s}{g*^{1/2}(x=1)} \tag{3.13}$$

Introducing then $\Delta = Y - Y_{eq}$, the Boltzmann equation becomes:

$$\Delta' = -Y'_{eq} - \frac{\lambda}{x^{n+2}}\Delta(\Delta + 2Y_{eq}) \tag{3.14}$$

and it can be studied the solution for early times and for late times.

- Early times ($1 < x < x_f$): $Y \simeq Y_{eq}$, so Δ and Δ' are of order 0

$$\Delta \simeq \frac{-Y'_{eq}x^{n+2}}{(2Y_{eq}+\Delta)\lambda} \simeq \frac{Y_{eq}x^{n+2}}{(2Y_{eq})\lambda} = \frac{x^{n+2}}{2\lambda}, \tag{3.15}$$

$$Y \simeq Y_{eq} + \frac{x^{n+2}}{2\lambda}. \tag{3.16}$$

- Late times ($x >> x_f$): $Y >> Y_{eq}$, so $\Delta \approx Y$ and Y, Y_{eq} can be neglected

$$\Delta' \simeq \frac{-\lambda}{z^{n+2}}\Delta^2, \tag{3.17}$$

integrating between x_f and $x > x_f$:

$$\frac{1}{\Delta} - \frac{1}{\Delta_f} = \frac{\lambda}{n+1}\left(\frac{1}{x_f^{n+1}} - \frac{1}{x^{n+1}}\right) \tag{3.18}$$

and we obtain:

$$Y = Y_{eq} + \left(\frac{\lambda}{n+1}\left(\frac{1}{x_f^{n+1}} - \frac{1}{x^{n+1}}\right) + \frac{1}{\Delta_f}\right)^{-1}. \tag{3.19}$$

If we consider $x \to \infty$:

$$\frac{1}{\Delta_\infty} - \frac{1}{\Delta_f} = \frac{\lambda}{n+1}\frac{1}{x_f^{n+1}} \tag{3.20}$$

Since Y decreases for a while thanks to the remaining interactions before becoming constant, we will have that $Y_f > Y_\infty$, so we can write:

$$Y_\infty \simeq \frac{n+1}{\lambda} x_f^{n+1}. \tag{3.21}$$

In order to write x_f, we should remember that at that point Y breaks away from Y_{eq}, and so it can be written $\Delta(x_f) = cY_{eq}(x_f)$, where c is an order unity constant. From the equation 3.15 for early times, we obtain:

$$\Delta(x_f) = \frac{Y_{eq}(x_f)x^{n+2}}{(2Y_{eq}(x_f) + \Delta(x_f))\lambda} \simeq \frac{x_f^{n+2}}{\lambda(2+c)} \tag{3.22}$$

and, applying the freeze out condition stated above, it can be written the equation:

$$\frac{x_f^{n+2}}{\lambda(2+c)} = cY_{eq}(x_f) = cax_f^{3/2}e^{-x_f}, \tag{3.23}$$

where $a = 0.145\frac{g}{g_{*s}}$. It can be found in an iterative way an approximate solution to this equation, that results:

$$x_f \simeq ln((2+c)\lambda ac) - \left(n + \frac{1}{2}\right) ln(ln((2+c)\lambda ac)). \tag{3.24}$$

The best choice, which gives the most precise fit with the numerical solution, is $c(c+2) = n+1$ [10], which yields:

$$\begin{aligned} x_f =& ln(0.038(n+1)(g/g_*^{1/2})M_P m_\Psi \sigma_0) - \\ &- \left(n + \frac{1}{2}\right) ln(ln(0.038(n+1)(g/g_*^{1/2})M_P m_\Psi \sigma_0) \end{aligned} \tag{3.25}$$

The value of x_f for some typical n, assuming m_ψ = 100GeV and $\sigma_0 \sim 10^{-38}cm^2$, corresponds to:

- $n = 0 \longrightarrow x_f \simeq 18$
- $n = 1 \longrightarrow x_f \simeq 15$
- $n = 2 \longrightarrow x_f \simeq 13$

and in figure 3.2 it have been plotted the different evolutions of the comoving density Y for these values of n, for both the numerical solution and the analytical one (that was presented above), together with the equilibrium distribution. It can be observed that, as was explained before, the comoving density tracks the equilibrium curve up to the freeze-out moment, when it becomes approximately constant. It should also be noted that increasing the value of n corresponds to the freeze-out happening earlier, resulting in an higher final amount of Y.

Finally, we can find the today's abundance of Ψ recalling that $n_{\Psi_0} = s_0 Y_\infty$, and thus

$$\begin{aligned} \Omega_{0\Psi} h^2 &= \frac{0.57 \cdot 10^9 (n+1) x_f^{n+1}}{\left(\frac{g*_s}{g*^{1/2}}\right) M_P \sigma_0} \\ &\approx O(1) \cdot (n+1) \left(\frac{x_f}{10}\right)^{n+1} \left(\frac{g*}{100}\right)^{1/2} \left(\frac{100}{g*_s}\right) \frac{10^{-38} cm^2}{\sigma_0} \end{aligned} \tag{3.26}$$

where in the last passage we have normalized with some typical values (note in particular the value for the cross section typical of weak interactions).

It can be observed that here there is no explicit dependence on the mass m_Ψ (just implicit inside x_f and g_*), and that there is inverse dependence on σ_0: the larger the cross section for annihilation, the smaller the final abundance of Ψ.

3.3 Conclusion

In this chapter we have reviewed the different evidences for the existence of dark matter, which manifest across a broad range of scales. These observations collectively build a convincing demonstration of the presence of a non-luminous, non-baryonic component that dominates the gravitational dynamics of the Universe.

We have also discussed about the WIMP (Weakly Interacting Massive Particle), that is one of the DM candidates of most interest - both for its presence in different theories of physics beyond the Standard Model and for the so called "WIMP miracle", consisting of the prediction of a relic abundance of WIMPs aligned with the observed dark matter density. Furthermore, we introduced the Boltzmann equations formalism, which underlies the description of the WIMP number density evolution in the early Universe.

In conclusion, in this chapter we addressed what makes of WIMPs an attractive possibility for explaining the dark matter problem, however many key questions regarding the precise nature and properties of dark matter are still unanswered. These open questions, together with the previously discussed

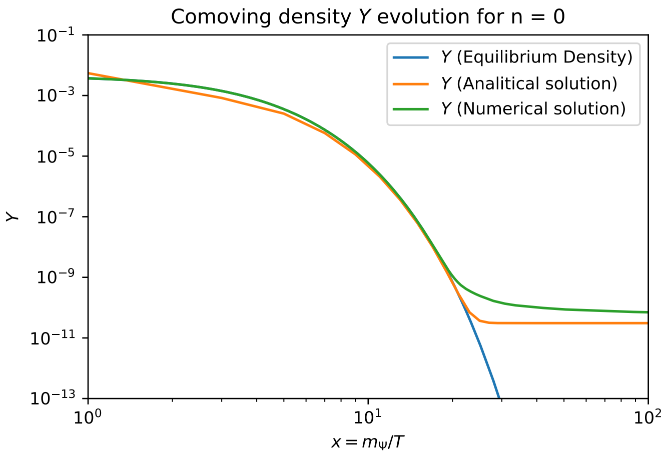

(a) $n = 0$

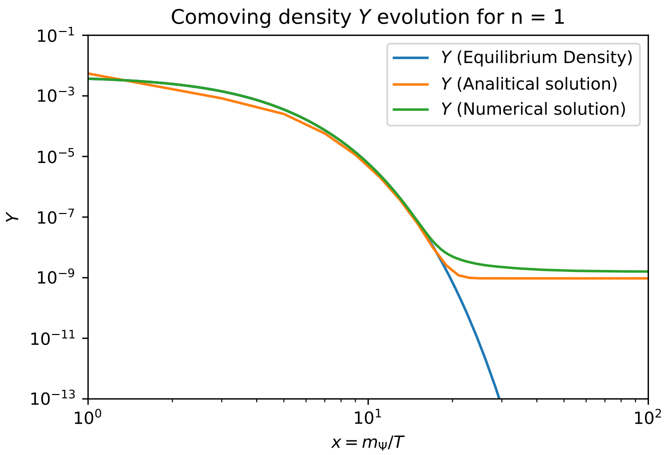

(b) $n = 1$

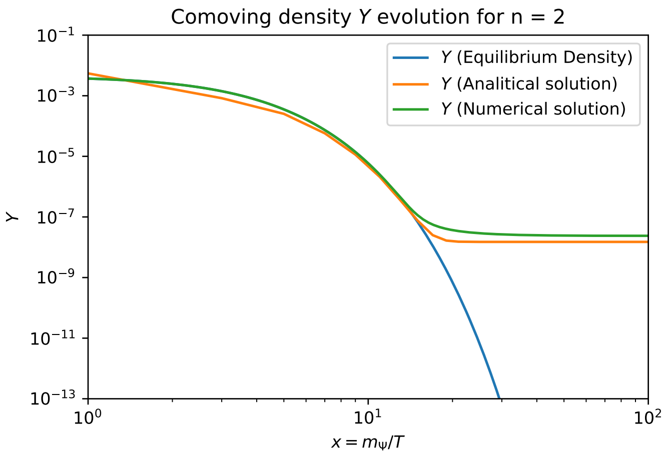

(c) $n = 2$

Figure 3.2: The blue line represent the equilibrium density Y_{eq}, while the green and orange lines correspond, respectively, to the numerical and analytical solutions of the Boltzmann equation.

baryon asymmetry problem, raise the intriguing possibility that both phenomena may have a common origin. This idea will be explored in the next chapter, where we examine the framework of WIMPy baryogenesis.

4

WIMPy Baryogenesis

WIMPy Baryogenesis is a mechanism that creates a link between WIMPs dark matter annihilation and production of a relic dark matter density, and the generation of a baryon asymmetry, under the assumption that WIMPs annihilations satisfy the Sakharov conditions. It will be shown that the amount of asymmetry generated through this mechanism strongly depends on some parameters, with a result that possibly differs of many orders of magnitude from the observed one.

An important piece of this puzzle are washout processes, that tend to delete the asymmetry, and the moment of their freeze-out (i.e. the moment in which their rate falls below expansion rate). The two main washout processes that will be considered here are inverse annihilations of baryons into DM and baryon-antibaryon scatterings. The importance of the freeze-out moment comes from the fact that a baryon asymmetry can be produced efficiently only once washout has become inefficient, so in order for this model to work out we would need their freeze-out to happen before WIMPs freeze-out. That moment is crucial also because the amount of WIMPs dark matter left will determine the value of the final baryon asymmetry.

When the baryons no longer have the energy needed to annihilate back into DM, inverse annihilations stop to be efficient, and this happens for $T < m_{DM}$. For the baryon-antibaryon scatterings, instead, the presence of an heavy exotic baryon field is needed in the processes, since they could in principle still occur efficiently at temperatures below m_{DM}.

Two conditions can be imposed on the mass of this exotic baryon field, present in all washout processes: it should be larger than m_{DM} in order that the scatterings already freezed out of at $T < m_{DM}$, but it should also allow the DM annihilation. It results:

$$2m_{DM} \geq m_{e.b.} \geq m_{DM}. \tag{4.1}$$

In DM annihilations SM particles (quarks) are produced, that carry a positive B, and the exotic baryon field, that carries the same baryon asymmetry, but negative. In order to avoid cancelling the asymmetry two possibilities are considered:

- Models where U(1) baryon symmetry is conserved: the exotic baryon field does have nonzero charge of a new discrete symmetry, while all SM particles don't, so it cannot decay into SM baryons modifying the asymmetry. Instead, it decays into sterile antibaryons, decoupled from the rest.

- Models where there is B-violating decay of the exotic baryon field into SM particles.

In the next sections WIMPy baryogenesis will be more deeply analyzed. In Section 4.1 a general presentation of the mechanism is provided, while Section 4.2 explores how the theoretical bounds on particle masses impact the expected baryon asymmetry. Finally, in Section 4.3 a specific realization of the mechanism is studied in detail, in which we propose the annihilation of dark matter directly into quarks. The section presents the interaction Lagrangian and possible decay channels of the new baryonic particle, and provides a numerical analysis of the Boltzmann equations governing the evolution of both the dark matter and baryon number abundances.

4.1 General theory

We will analyze a model in which DM species X annihilate violating the baryon number and producing a quark and another particle ψ_i (or more than one). The full Boltzmann equations to describe the abundances of the different species depend on the specific model, but for the cases we are interested in, where WIMPs annihilations are the main responsible of baryogenesis, it is sufficient to consider two terms: one regarding DM annihilation and B production, and another regarding B-violating washout scatterings that tend to balance the asymmetry. As already seen in the previous sections, the Boltzmann equations will be written in terms of the adimensional quantities $Y_i = n_i/s$ and $x = m_X/T$.

For the dark matter number density, the evolution equation that we'll consider is very similar to the conventional equation for WIMPs, that has been presented in section 3.2:

$$\frac{dY_X}{dx} = -\frac{2s(x)\langle\sigma_{ann}|v|\rangle}{xH(x)}(Y_X^2 - (Y_X^{eq})^2). \tag{4.2}$$

Here it could have been added also an additional back reaction term, accounting for the presence of a baryon asymmetry that modifies the inverse scattering rate, but it has been neglected since it is proportional to the baryon asymmetry $Y_{\Delta B} << 1$ (this approximation simplifies the system decoupling the equations for Y_X and $Y_{\Delta B}$).

For the Baryon asymmetry the Boltzmann equation is:

$$\frac{dY_{\Delta B}}{dx} = \frac{\epsilon\, s(x)}{x\, H(x)}\,\langle\sigma_{ann}|v|\rangle(Y_X^2 - (Y_X^{\text{eq}})^2) - \frac{s(x)}{x\, H(x)}\,\langle\sigma_{wa}|v|\rangle\,\frac{Y_{\Delta B}}{2\, Y_\gamma}\prod_i Y_i^{eq} \tag{4.3}$$

The first term consists in the difference of X annihilations into baryons and into antibaryons: ϵ is the fractional asymmetry that is generated at each interaction, while the rest corresponds to the annihilation rate. The second term is the washout term, here σ_{wa} is the cross section of washout processes and $\mu_{\Delta B}/T$ has been rewritten as $Y_{\Delta B}/2Y_\gamma$ (B.15). A full derivation of these two Boltzmann equations can be found in the appendix B.3.

It could be considered here also a term accounting for scatterings between the exotic baryon field and WIMPs, but it would be $\propto Y_{e.b.}^{eq} Y_X$ and it can be safely ignored with respect to the other washout terms. In our treatment X is the only particle species that is not in equilibrium.

Equation 4.3 yields an integral solution:

$$
\begin{aligned}
Y_{\Delta B}(x) = &\int_0^x dx' \, \frac{\epsilon \, s(x')}{x' \, H(x')} \, \langle \sigma_{\text{ann}} |v| \rangle (Y_X^2 - \left(Y_X^{\text{eq}}\right)^2)(x') \cdot \\
&\cdot \exp\left[- \int_{x'}^{x} dx'' \, \frac{s(x'')}{x'' 2Y_\gamma \, H(x'')} \, \langle \sigma_{\text{wa}} |v| \rangle \prod_i Y_i^{\text{eq}}(x'') \right] \approx \\
&\approx -\frac{\epsilon}{2} \int_0^x dx' \, \frac{dY_X(x')}{dx'} \exp\left[- \int_{x'}^{x} dx'' \, \frac{s(x'')}{x'' 2Y_\gamma \, H(x'')} \, \langle \sigma_{\text{wa}} |v| \rangle \prod_i Y_i^{\text{eq}}(x'') \right] = \\
&= -\frac{\epsilon}{2} \int_0^x dx' \, \frac{dY_X(x')}{dx'} \exp\left[- \int_{x'}^{x} dx'' \, \frac{\Gamma_{wa}}{x'' H(x'')} \right],
\end{aligned} \tag{4.4}
$$

where in the last passage we have defined the washout rate:

$$
\Gamma_{wa} \equiv \frac{s(x)}{2Y_\gamma} \, \langle \sigma_{\text{wa}} |v| \rangle \prod_i Y_i^{\text{eq}}(x). \tag{4.5}
$$

We can observe an exponential term that tries to cancel the baryon asymmetry produced by the first term dY_X/dx, which becomes different from zero when x starts to be ≥ 1 (there is exit from equilibrium that results in net B formation).

The freeze out of washout processes happens when the ratio Γ_{wa}/H becomes smaller than 1. The term Γ_{wa} can be modeled as a simple step function if it rapidly decreases with x (for example if Y_i^{eq} has an exponential decrease when m_i/T becomes large): what happens is that up a a critical value of x - typically the washout freeze out, that will be referred to as x_{washout} - the integral is large enough to make the exponential very small, suppressing the asymmetry. Above that value of x, the washout rate has a strong decrease so that the integrand becoming smaller than 1 makes it possible to approximate the exponential to 1. This leads to:

$$
Y_{\Delta B}(\infty) \approx -\frac{\epsilon}{2} \int_{x_{\text{washout}}}^{\infty} dx' \, \frac{dY_X(x')}{dx'} = \frac{\epsilon}{2} \left[Y_X(x_{\text{washout}}) - Y_X(\infty) \right]. \tag{4.6}
$$

From this result we can see that the baryon asymmetry is proportional to the efficiency ϵ of each WIMPs annihilation, times their total number after the washout processes freezed out.

At late times it can be proven that $Y_X(\infty) \approx \frac{5GeV}{m_X} Y_{\Delta B}(\infty)$[1] ($Y_{\Delta B}(\infty)$ is observed to be of order $\sim 9 \cdot 10^{-11}$ [11]), so, considering a kind of dark matter having weak-scale mass[2], it should be $Y_X(\infty) < Y_{\Delta B}(\infty)$. Since $\epsilon < 1$ we obtain the condition $Y_X(x_{\text{washout}}) >> Y_X(\infty)$, meaning that to produce a large enough ΔB washout processes should freeze out before WIMPs annihilations freeze out. In terms of parameters of the system, there are two conditions that allow to implement this. It should be considered the ratio between the washout rate $\Gamma_{wa}(x)$ (4.5) and the WIMPs annihilation rate

$$\Gamma_{WIMP}(x) = 2s(x)\langle\sigma_{ann}|v|\rangle Y_X(x), \tag{4.7}$$

which is:

$$\frac{\Gamma_{\text{wa}}(x)}{\Gamma_{\text{WIMP}}(x)} \approx \frac{\langle\sigma_{\text{washout}} v\rangle \prod_i Y_i^{\text{eq}}(x)}{4\,\langle\sigma_{\text{ann}} v\rangle\, Y_{\text{X}}^{\text{eq}}(x)\, Y_\gamma} \tag{4.8}$$

The requirement translates to $\frac{\Gamma_{\text{washout}}(x)}{\Gamma_{\text{WIMP}}(x)} < 1$ at x_{washout}, which is true if one of the baryon fields is more massive than DM ($\prod_i Y_i^{\text{eq}}(x)/Y_{\text{X}}^{\text{eq}}(x)\, Y_\gamma << 1$) or if $\langle\sigma_{ann}|v|\rangle >> \langle\sigma_{wa}|v|\rangle$, but this last condition is less probable because the B-violating couplings appearing in one cross section are the same that appear in the other, plus the fact that asking for a very small value of $\langle\sigma_{wa}|v|\rangle$ corresponds to a too small value of ϵ, as will be shown below.

4.2 Baryon asymmetry expectations

It is here determined which range of values for the baryon asymmetry can be achieved in WIMPy baryonesis models. The mass of the dark matter particle X will be taken to be of order $O(\text{TeV})$, and in this section the annihilation process that will be considered is the simplest case:

$$XX \longrightarrow Q\psi \tag{4.9}$$

[1]It is measured that today the densities of dark matter and baryons differ by a factor 5: $\rho_X(t_0) = 5\rho_{\Delta B}(t_0)$. Since the density can be written as function of the adimensional quantity Y, $\rho(t_0) = mn(t_0) = mY(\infty)s(t_0)$ (for baryons it can be used the mass of the proton, $O(\text{GeV})$), it can be derived the relation $Y_X(\infty) \approx \frac{5GeV}{m_X} Y_{\Delta B}(\infty)$.

[2]Here and in the following, the X mass can be considered to be $m_X \sim$TeV.

where Q is a generic quark of the SM, while ψ is the exotic baryon field, which was mentioned above as a necessary component of this theory.

From the previous section we know that for the final baryon asymmetry to be large we would need the freeze out of washout processes to happen well in advance of the WIMPs freeze out, when they are still present in a large number, and this happens if the exotic baryon field is massive enough with respect to the X particles.

For both the upper and lower limits of the baryon asymmetry range that will be estimated, it will be computed the baryon asymmetry value and the DM-baryons energy density ratio.

- **Upper limit**: As we just stated, in order to obtain a large baryon asymmetry the mass of the exotic baryon field should be larger than m_X ($m_\psi \gtrsim m_X$). To estimate an upper limit, we should consider the kinematical limit to the WIMPs annihilations: $m_\psi < 2m_X$; this limits the time at which the washout processes freeze out with respect to the time at which the annihilations of WIMPs freeze out, which translates into the maximum possible amount of WIMPs remaining after washout freezes out. These two timescales are respectively referred to as $x_{\text{washout}} = \dfrac{m_X}{T_{\text{washout}}}$ and $x_{\text{ann}} = \dfrac{m_X}{T_{\text{ann}}}$, and they govern the resulting baryon asymmetry both in the upper and lower limit cases.

  Being $x_{\text{washout}} \approx x_{\text{ann}} \dfrac{m_X}{m_\psi}$, and since we know that the point of WIMP annihilations freeze out x_{ann} takes place at $T_{\text{ann}} \sim m_X/30$ (for an O(TeV) DM mass), it results that $x_{\text{washout}} \gtrsim 15$. We can then write the maximum value for the baryon asymmetry:

$$Y_{\Delta B}(\infty) \approx \frac{\epsilon}{2} Y_X(x_{\text{washout}}) < \frac{\epsilon}{2} Y_X^{eq}(15) \approx \epsilon \times 10^{-8}, \tag{4.10}$$

  where in the first passage it has been applied the condition of WIMPs annihilations freeze out after washout freeze out, that was derived in the previous section from equation 4.6 [3]. It can be noted from 4.10 that the result is dependent on x_{washout} and so on the ratio between m_X and m_ψ rather than on the single masses: the smaller the ratio, the larger the generated baryon asymmetry would be.

[3]The approximation done comes from the condition $Y_X(x_{\text{washout}}) >> Y_X(\infty)$.

We would like to find now the ratio between the baryons and the WIMPs energy densities, that can be written as:

$$\frac{\Omega_B}{\Omega_X} = \frac{m_p Y_{\Delta B}(\infty)}{m_X Y_X(\infty)} \approx \frac{\epsilon}{2}\frac{Y_X(x_{\text{washout}})}{Y_X(x_{\text{ann}})}\left(\frac{GeV}{m_X}\right) \approx \frac{\epsilon}{2}\frac{Y_X^{eq}(15)}{Y_X^{eq}(30)}\left(\frac{GeV}{m_X}\right), \tag{4.11}$$

where m_p stands for the mass of the proton. Here we have used the fact that the final WIMPs number density $Y_X(\infty)$ does not decrease much after the annihilations freeze out, and so it is almost equal to $Y_X(x_{\text{ann}})$ and to the equilibrium value at $x = 30$, $Y_X^{eq}(30)$.

Since we would like to find an upper limit also for this ratio we can consider some typical values for the parameters, and taking a weak-scale mass $m_X \sim$ TeV, $O(1)$ couplings, and a baryon asymmetry efficiency of order $\epsilon \sim 10^{-2}$ [6], what we obtain is:

$$\frac{\Omega_B}{\Omega_X} \lesssim 10\left(\frac{\epsilon}{10^{-2}}\right)\left(\frac{TeV}{m_X}\right). \tag{4.12}$$

Thus, it could result an overabundance of baryons over dark matter that in the limiting case would be of one order of magnitude.

- **Lower limit**: To estimate a lower bound to the range of values that the asymmetry can take in this theory, it should be considered the opposite situation: the case in which WIMPs annihilations exit from equilibrium before washout processes freeze out. This situation is achieved if $m_\psi << m_X$, and we already know that in this case the amount of dark matter present at the moment of washout freeze out is not sufficient to provide the observed baryon asymmetry, according to equation 4.6. However, if we consider that in this case the real abundance of dark matter strongly deviates from the equilibrium value, that is much lower, annihilations can still take place after washout freeze out, but not in a significant amount to noticeably affect the value of Y_X after x_{ann}. These residual annihilation processes, though, can be responsible of a non-zero baryon asymmetry.

  In order to compute the baryon asymmetry, from equation 4.6, we are interested in the difference between the WIMPs number densities at x_{washout} and at ∞, which can be found by integrating the Boltzmann equation for

WIMPs (4.2) inside this range. Since for $x > x_{\text{ann}}$ the equilibrium density is very small with respect to Y_X, the Boltzmann equation can be written as:

$$\frac{dY_X}{dx} \approx -\frac{2\,s(x)}{x\,H(x)}\,\langle\sigma_{\text{ann}}\,|v|\rangle\,Y_X^2\,. \tag{4.13}$$

Moreover, to simplify the integration, we can consider the averaged cross section to be constant in our interval, and we can evaluate $s(x)$ and $H(x)$ at x_{ann} putting in evidence that the dependence on x is just:

$$\frac{s(x)}{x\,H(x)} = \frac{s(x_{\text{ann}})}{H(x_{\text{ann}})}\,\frac{x_{\text{ann}}}{x^2}\,, \tag{4.14}$$

so equation 4.13 becomes:

$$\frac{dY_X}{dx} \approx -\frac{2\,s(x_{\text{ann}})}{H(x_{\text{ann}})}\,\langle\sigma_{\text{ann}}\,|v|\rangle\,Y_X^2\,\frac{x_{\text{ann}}}{x^2}\,. \tag{4.15}$$

Then, because Y_X changes little between the values of x we are interested in $(x_{\text{washout}}, \infty)$, we can approximate it with $Y_X(x_{\text{ann}})$ and treat Y_X^2 as a constant in the integration. It results:

$$Y_X(x_{\text{washout}}) - Y_X(\infty) \approx \frac{2\,s(x_{\text{ann}})}{H(x_{\text{ann}})}\,\langle\sigma_{\text{ann}}\,|v|\rangle\,Y_X(x_{\text{ann}})^2\,\frac{x_{\text{ann}}}{x_{\text{washout}}}\,. \tag{4.16}$$

It is possible to recognize in the right hand side of the equation the rate of WIMPs annihilations $\Gamma_{\text{WIMP}}(x_{\text{ann}})$ as defined in 4.7, and recalling that x_{ann} is the point at which the rate of WIMPs annihilations equates the universe expansion rate, equation 4.16 can be written as:

$$Y_X(x_{\text{washout}}) - Y_X(\infty) \approx \frac{2\,x_{\text{ann}}}{x_{\text{washout}}}\,Y_X(x_{\text{ann}}) \approx \frac{2\,x_{\text{ann}}}{x_{\text{washout}}}\,Y_X(\infty)\,. \tag{4.17}$$

The baryon asymmetry in this case then results:

$$Y_{\Delta B} \approx \epsilon\,\frac{x_{\text{ann}}}{x_{\text{washout}}}\,Y_X(\infty) \approx \epsilon\left(\frac{m_\psi}{m_X}\right)Y_X(\infty)\,, \tag{4.18}$$

where we have used the fact, already highlighted in the upper limit case, that $x_{\text{washout}} \approx x_{\text{ann}}\dfrac{m_X}{m_\psi}$.

The corresponding ratio between energy densities is:

$$\frac{\Omega_B}{\Omega_X} \approx \frac{m_p\, Y_{\Delta B}(\infty)}{m_X\, Y_X(\infty)} \sim 10^{-3}\, \epsilon \left(\frac{m_\psi}{m_X}\right)\left(\frac{\text{TeV}}{m_X}\right). \tag{4.19}$$

We can observe that both these results are linearly dependent on the exotic baryon mass: the smaller its value with respect to the WIMPs mass, the smaller the generated baryon asymmetry. Considering some typical values for the parameters, as we did in the previous case, allow to obtain a lower value for the estimated ratio:

$$\frac{\Omega_B}{\Omega_X} \gtrsim 10^{-6}\left(\frac{\epsilon}{10^{-2}}\right)\left(\frac{TeV}{m_X}\right), \tag{4.20}$$

where it has been assumed that the condition on the masses $m_\psi << m_X$ is not too strong, so for example $m_\psi/m_X \gtrsim 10^{-1}$ (both dark matter and the new exotic baryon are taken to have weak scale masses). This result however can be even lower, as it is clear from the arbitrariness of the masses hierarchy and the ϵ value choice, which depends on the imaginary parts of the couplings.

In conclusion, while generic WIMPy baryogenesis models don't predict a precise value for the baryon-to-dark matter ratio, they restrict the possible range to:

$$10^{-6} \lesssim \frac{\Omega_B}{\Omega_X} \lesssim 10, \tag{4.21}$$

that includes the observed value ~ 0.2, which however is nearer to the upper bound.

4.3 Model of WIMP Annihilation to Quarks

In this section it will be presented a model of baryogenesis in which pairs of dark matter particles, here corresponding to gauge singlet Dirac fermions called as above X and $\bar{X}$, annihilate into quarks producing directly a baryon asymmetry.

It could be considered also an alternative model in which the annihilation of WIMPs produces leptons, and consequently a lepton asymmetry, that is later converted to a baryonic one via sphaleron transitions. However, this model presents some complications due to the fact that the generated lepton asymmetry should be large enough before the electroweak phase transition takes place, at which point sphalerons cease to be efficient, and this translates to lower bounds on the masses. Therefore, we will focus only on the first model.

4.3.1 Overview

This model, in addition to the dark matter particles X and $\bar{X}$, involves the presence of singlet scalars S_α[4], and vectorlike exotic quark color triplets ψ_i and $\bar{\psi}_i$. The process consists in the annihilation of the WIMPs into S_α, which then decays to a quark and the new field ψ_i: this is described by the Lagrangian[5]

$$\mathcal{L} = \mathcal{L}_{\text{kin}} + \mathcal{L}_{\text{mass}} - \frac{i}{2}(\lambda_{X_\alpha} X^2 + \lambda'_{X_\alpha} \bar{X}^2) S_\alpha + i\lambda_{B_\alpha} S_\alpha \bar{u}\psi + h.c. \tag{4.22}$$

To have the CP violation imposed by the Sakharov conditions, it is required λ_{B_α} to be complex, and the existence of more than one scalar S (from which we write the subindex α) that allows to have a relative phase in the different amplitudes.

The baryon asymmetry in the Standard Model sector is generated in the quark, while a corresponding opposite asymmetry is generated in the exotic baryon. To be coherent both with particle physics bounds about the stability of free colored particles, and with cosmological observations that limit massive stable particles abundances to avoid Universe overclosure, we would expect these exotic baryons to decay, and care must be taken that decaying they do not erase the baryon asymmetry built in $\bar{u}$ with the WIMPs annihilations.

We assume the presence of a new symmetry Z_4, which features charges of the fields as in table 4.1.

It can be observed that this symmetry guarantees the stability of dark matter, and also the stability of protons. If $m_p < 2m_X$ and $m_p < m_S$, indeed, their overall Z_4 charge being -1 doesn't allow them to decay into lighter mesons or leptons, which have charge $+1$.

[4]We assume S_α to have weak scale masses.

[5]The fermionic fields that appear in this Lagrangian are two components Weyl fields; this formalism is used in this section for consistency with the literature (it is the one adopted in [6]). Therefore, here $\bar{u}$ is a left-handed Weyl fermion.

	X	$\bar{X}$	ψ	$\bar{\psi}$	S	$\bar{u}$	$\bar{d}$	$\phi/\tilde{d}$	Q	H	n	Leptons
Z_4	+i	-i	+1	+1	-1	-1	-1	-1	-1	+1	+1	+1

Table 4.1: Charges of the fields under the Z_4 symmetry

For the decay of the ψ field, two scenarios are to be considered, both of them allowed by the Z_4 symmetry and consisting in the production of a singlet n along with quarks.

- The first scenario predicts a baryon-number conserving decay of ψ into a sterile sector decoupled from Standard Model at low energies, thereby keeping the negative baryon asymmetry produced in ψ inside this sector. The products of this decay would be two SM quarks and a singlet n_i which carries non-zero baryon number; this would occur via the mediation of a new colored scalar that we denote by ϕ[6]. The Lagrangian would thus include a term of the form:

$$\Delta\mathcal{L} = \lambda_i \bar{\psi}_i \bar{d}_i \phi^* + \lambda_i' \phi \bar{d}_i n_i + h.c. \tag{4.23}$$

- According to the second scenario, instead, ψ would undergo a baryon-number violating decay which generates a net baryon asymmetry, with no counterpart in a decoupled sector. The products would still be two SM quarks and a singlet n, with the latter being now a Majorana fermion that carries no baryon number. The mediator of ψ decays, here, would be another new colored scalar, $\tilde{d}_i$[7], and the new term in the Lagrangian would be:

$$\Delta\mathcal{L} = \lambda \epsilon^{ijk} \bar{\psi}_i \bar{d}_j \tilde{d}_k^* + \lambda_i' \bar{d}_i \tilde{d}_i n + h.c. \tag{4.24}$$

The Z_4 symmetry, besides not allowing ψ to decay solely to quarks[8], ensures that terms such as $QH\bar{\psi}$, which could cancel the baryon asymmetry, are forbidden.

[6] ϕ would have representation $(3, 1, -\frac{1}{3})$ under the SM gauge groups $SU(3)_C \times SU(2)_L \times U(1)_Y$.

[7] $\tilde{d}_i$ would have representation $(3, 1, -\frac{1}{3})$ under the SM gauge groups $SU(3)_C \times SU(2)_L \times U(1)_Y$. In supersymmetric models, the new components that appear in this Lagrangian could be the down squark $\tilde{d}$ and the neutralino n.

[8] Terms such as $\phi^* \bar{d}\bar{u}$ and $\tilde{d}^* \bar{d}\bar{u}$ in the Lagrangian are forbidden by the symmetry Z_4.

4.3.2 Generation of the asymmetry and washout processes

The processes that are responsible of the asymmetry generation in this model are depicted in figures 4.1 and 4.2, and consist in the decay of the pseudoscalar S_α and in the annihilation of X particles, both having as final states $\bar{u}\psi$ and their conjugates. We can see represented not only the tree-level, but also the one-loop diagrams because the violation of CP that is needed to satisfy the Sakharov conditions comes from the interference between the two.

To simplify the analysis ad avoid taking into account all the possible baryon final states, we assume that in our model the only coupling between the scalar S_α and a quark to be different from zero is the one with the u (and its antiparticle), which causes WIMPs to annihilate dominantly into this quark flavor.

Another assumption to ease the model can be done regarding the scalars S_α. As we pointed out earlier two different scalars are needed to produce CP violation, but we could consider the processes of our interest taking place mainly through the lightest scalar, that we call S_1. Our assumption is that the cross sections of processes involving S_1 are more than 5 times larger than the cross sections involving S_2, which gives:

$$\frac{\lambda_{B_2}^4}{m_{S_2}^4} \lesssim \frac{\lambda_{B_1}^4}{5m_{S_1}^4}, \tag{4.25}$$

$$\frac{\lambda_{X_2}^2 \lambda_{B_2}^2}{m_{S_2}^4} \lesssim \frac{\lambda_{X_1}^2 \lambda_{B_1}^2}{5m_{S_1}^4}, \tag{4.26}$$

and to further simplify the computations we also assume that the mass of the scalar S_2 is much larger than the mass of S_1.

With these premises, it can be found a simple form to express the asymmetry factors for the decay of S_1

$$\epsilon_1 = \frac{\Gamma(S_1 \to \psi_i \bar{u}_i) - \Gamma(S_1 \to \psi_i^\dagger \bar{u}_i^\dagger)}{\Gamma(S_1 \to \psi_i \bar{u}_i) + \Gamma(S_1 \to \psi_i^\dagger \bar{u}_i^\dagger)} \tag{4.27}$$

and for the XX annihilation

$$\epsilon_2 = \frac{\sigma(XX \to \psi_i \bar{u}_i) + \sigma(\bar{X}\bar{X} \to \psi_i \bar{u}_i) - \sigma(XX \to \psi_i^\dagger \bar{u}_i^\dagger) - \sigma(\bar{X}\bar{X} \to \psi_i^\dagger \bar{u}_i^\dagger)}{\sigma(XX \to \psi_i \bar{u}_i) + \sigma(\bar{X}\bar{X} \to \psi_i \bar{u}_i) + \sigma(XX \to \psi_i^\dagger \bar{u}_i^\dagger) + \sigma(\bar{X}\bar{X} \to \psi_i^\dagger \bar{u}_i^\dagger)}, \tag{4.28}$$

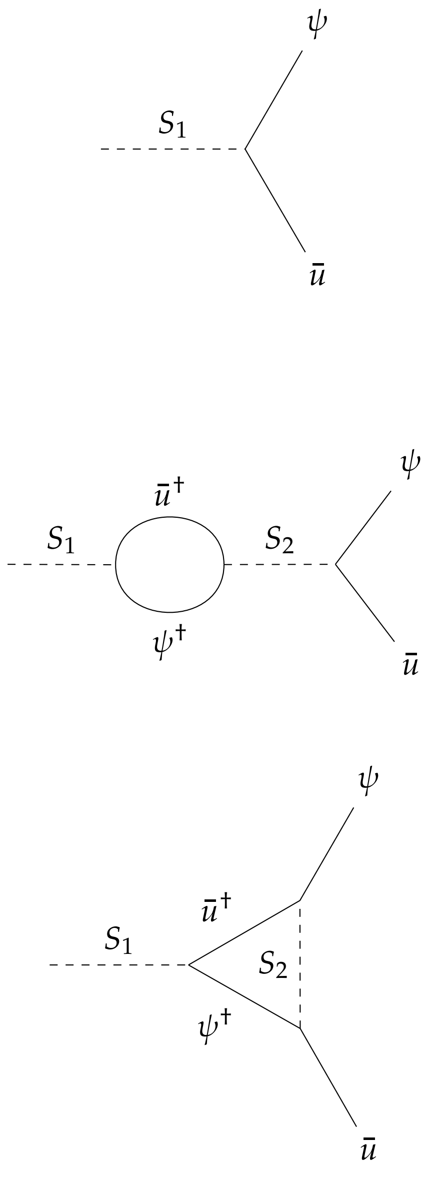

Figure 4.1: Feynman diagrams representing S decay at tree level and one loop level.

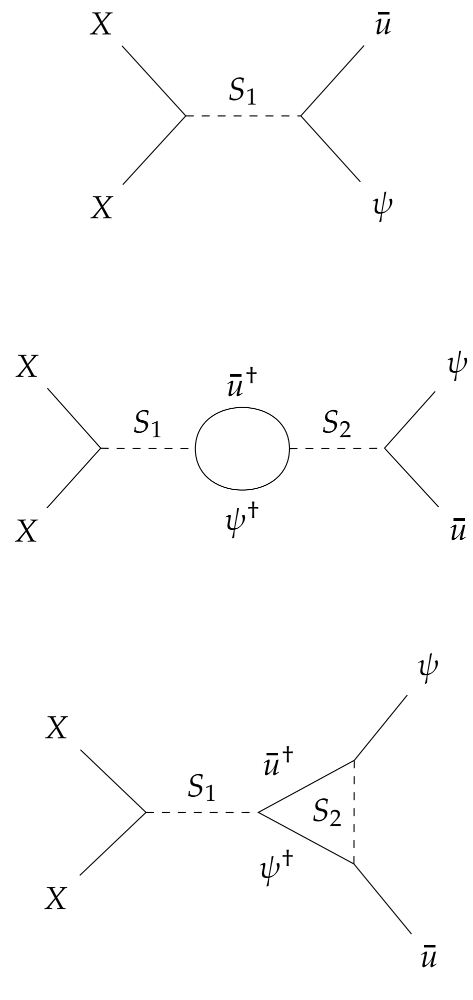

Figure 4.2: Feynman diagrams representing XX annihilation at tree level and one loop level.

which, between the two, is the process of greatest interest to us. This last factor, in fact, can be expressed as [6]:

$$\epsilon_2 \approx -\frac{1}{6\pi}\frac{\mathrm{Im}(\lambda_{B_1}^2\lambda_{B_2}^{*2})}{|\lambda_{B_1}|^2}\frac{(2m_X)^2}{m_{S_2}^2}\left[7-15\left(\frac{m_\psi}{2m_X}\right)^2+9\left(\frac{m_\psi}{2m_X}\right)^4-\left(\frac{m_\psi}{2m_X}\right)^6\right]. \quad (4.29)$$

It can be observed that ϵ is proportional to $(2m_X)^2$, which corresponds to the momentum in the S_1 propagator in WIMPs annihilations[9], and inversely proportional to $m_{S_2}^2$. If $m_\psi = 2m_X$, the asymmetry factor becomes zero: this coincides with a kinematic point where the energy available from XX annihilation is not sufficient for the particles running in the loop (ψ and u) to go on-shell, which is a necessary condition for having an imaginary part in the loop amplitude and therefore CP violation. We can find an upper bound to ϵ:

$$|\epsilon_2| \leq \frac{2\lambda_{B_1}^2}{3\pi\sqrt{5}}\frac{m_X^2}{m_{S_1}^2}\left[7-15\left(\frac{m_\psi}{2m_X}\right)^2+9\left(\frac{m_\psi}{2m_X}\right)^4-\left(\frac{m_\psi}{2m_X}\right)^6\right] \quad (4.30)$$

where, besides applying 4.25 and 4.26, large physical CP phases have been assumed, which allows the approximation $\mathrm{Im}(a) \approx a$, with a denoting a product of couplings.

The same expression could have been written for the decay of S_1 substituting $2m_X$ with m_{S_1}. We know from the previous discussion that the final asymmetry is proportional to $Y_X(x_{\mathrm{washout}})$, or $Y_S(x_{\mathrm{washout}})$ for the case of S decays, so there is an inverse dependence on the masses. If we assume that XX annihilations are the most relevant process in the asymmetry generation, i.e. the baryon asymmetry produced by annihilations is larger than the asymmetry produced by S decays, we should then require that $m_X < m_S$.

As we already stressed in section 4.1, the final baryon asymmetry is also strongly influenced by the washout processes. The washout processes for our model are inverse annihilations, scatterings between quarks and antiquarks, and $\psi X \to uX$ interactions, however, being these last processes Boltzmann suppressed and the inverse annihilations not kinematically allowed for $T < m_X$, the main contribution to washout comes from the scatterings $\bar{u}\psi \leftrightarrow \bar{u}^\dagger\psi^\dagger$

[9]The momentum that flows in the propagator is $\sqrt{\hat{s}} = 2m_X + O(T)$, with $T << m_X, m_{S_1}$ at freeze out.

(displayed in figure 4.3).

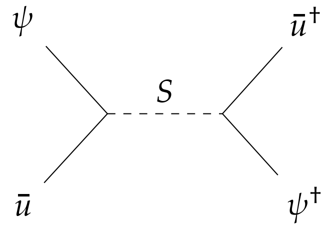

(a) s-channel

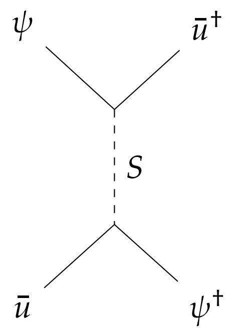

(b) t-channel

Figure 4.3: Feynman diagrams of the interactions $\bar{u}\psi \leftrightarrow \bar{u}^\dagger\psi^\dagger$ contributing to baryon number washout.

As we pointed out previously, to have a large enough final baryon asymmetry we need these washout processes to become inefficient prior to WIMPs annihilations, and this implies that $\Gamma_{\rm wa}$ must be smaller than $\Gamma_{\rm WIMP}$ at washout freeze-out.

The generic form of the washout rate (4.5) that was presented in section 4.1 can now be expressed for the dominant washout process in our model:

$$\Gamma_{\rm wa}(x) \approx \frac{s(x)}{2Y_\gamma}\langle \sigma_{\bar{u}\psi\to\bar{u}^\dagger\psi^\dagger} v\rangle Y_u^{\rm eq} Y_\psi^{\rm eq}(x). \tag{4.31}$$

The condition of 4.31 being smaller than $\Gamma_{\rm WIMP}$ can be implemented in two ways: one way could be the cross-section that appears in $\Gamma_{\rm wa}$ being small with respect to the one appearing in Γ_{WIMP}, which would require small couplings $\lambda_B << 1$. However, this would limit the asymmetry generation, since this condition suppresses the asymmetry factor ϵ (as can be seen in 4.30). The other option, which is therefore preferable, is that $m_\psi \gtrsim m_X$, implying that while DM is annihilating the abundance $Y_\psi^{eq}(x_{\text{washout}})$ is Boltzmann suppressed.

4.3.3 Numerical analysis: evolution of abundances and parameters dependence

To conclude the discussion of the model and its implications for baryon asymmetry generation, we present here a set of numerical results that illustrate the behavior of the key quantities involved and highlight the sensitivity to the model parameters λ_X and λ_B. These results were obtained through direct numerical integration of the Boltzmann equations derived earlier.

All simulations refer specifically to the WIMP annihilation scenario into quarks plus by a new heavy baryonic state, as presented in this section. The choice of particle masses respects the constraints derived from the requirement of successful baryogenesis, namely that the washout processes must freeze out before the annihilation of the WIMPs is complete (4.1), and the constraint on the dominance of XX annihilations over S decays in the net B production ($m_S > m_X$).

The first plot (figure 4.4) compares the comoving WIMPs abundance Y_X obtained from the numerical solution of the Boltzmann equation 4.2, with the corresponding analytical approximation that is the same[10] used in Section 3.2 of the chapter about Dark Matter. For completeness, also the equilibrium distribution is present in the plot. The good agreement between the two in the early stages confirms the validity of the approximation under suitable conditions.

Subsequently, a contour plot of the final value of Y_X as a function of λ_B and λ_X is shown (figure 4.5). The dependence on the couplings is to be searched in the value of the annhilation cross-section: $\sigma_{\text{ann}} \propto \lambda_X^2 \lambda_B^2$. This visualization is particularly useful for identifying the region of parameter space that leads to a WIMPs final number density compatible with the observed Dark Matter relic density. The isolines help guide the choice of parameters in a phenomenologically viable region.

Finally, we include the evolution of the baryon asymmetry $Y_{\Delta B}$, derived by

[10] Up to a factor 2.

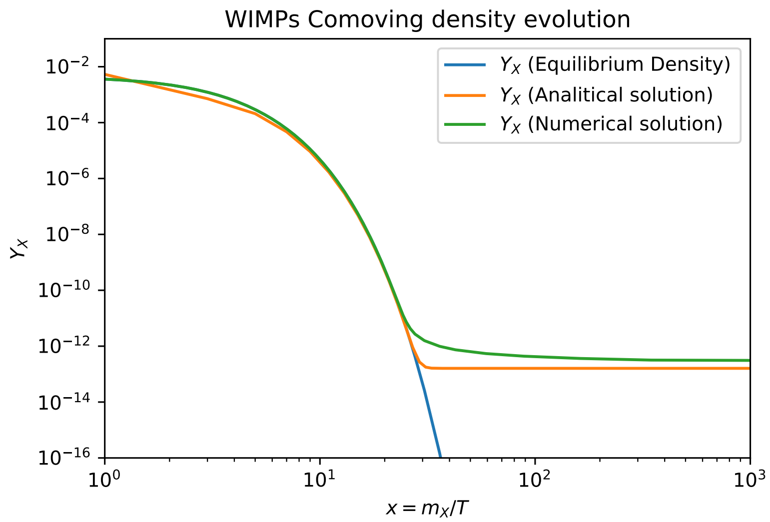

Figure 4.4: WIMPs comoving abundance Y_X and analytical solution, compared with the equilibrium evolution. The model parameters used to obtain these density lines are: $m_X = 4.25$ TeV, $m_\Psi = 7.25$ TeV, $m_S = 5$ TeV, $\lambda_X = 3.5$, $\lambda_B = 5.5$. The value of the annihilation cross-section is computed considering only the tree-level (see fig. 4.2), and it results $\sigma_{\text{ann}} = 5.43 \times 10^{-10}\text{GeV}^{-2} \simeq 6.29 \times 10^{-27}$ cm^3/s. We have also have assumed the thermally averaged cross-section to be independent from the velocity ($n = 0$). The freeze-out temperature corresponds to $x_f \sim 24$. The analytic prediction yields $Y_X^{\text{analytic}}(\infty) = 1.61 \times 10^{-13}$ (from equation 3.21), while the numerical result gives $Y_X(\infty) = 2.98 \times 10^{-13}$.

solving numerically the Boltzmann equation 4.3, adapted to our model of WIMP annihilation to quarks:

$$\frac{dY_{\Delta B}}{dx} = \frac{\epsilon\, s(x)}{x\, H(x)} \langle \sigma_{ann} |v| \rangle (Y_X^2 - (Y_X^{\text{eq}})^2) - \frac{s(x)}{x\, H(x)} \langle \sigma_{\bar{u}\psi \to \bar{u}^\dagger \psi^\dagger} v \rangle \frac{Y_{\Delta B}}{2\, Y_\gamma} Y_u^{\text{eq}} Y_\psi^{\text{eq}}(x). \tag{4.32}$$

As already pointed out, this is an approximate expression, which neglects back reaction terms and considers only baryon-antibaryon scatterings to be primarily responsible for the washout effects. Moreover, as for the previous plots, it has been used a simplified annihilation cross section that takes into account only the tree level of 4.2. While this result is based on a simplified treatment and is therefore less precise, it provides a qualitative understanding of the dynamics of asymmetry generation in this scenario. We can indeed observe that, starting from a symmetric condition, the asymmetry rapidly increases and then, with the departure from equilibrium of WIMPs annihilations, it nearly

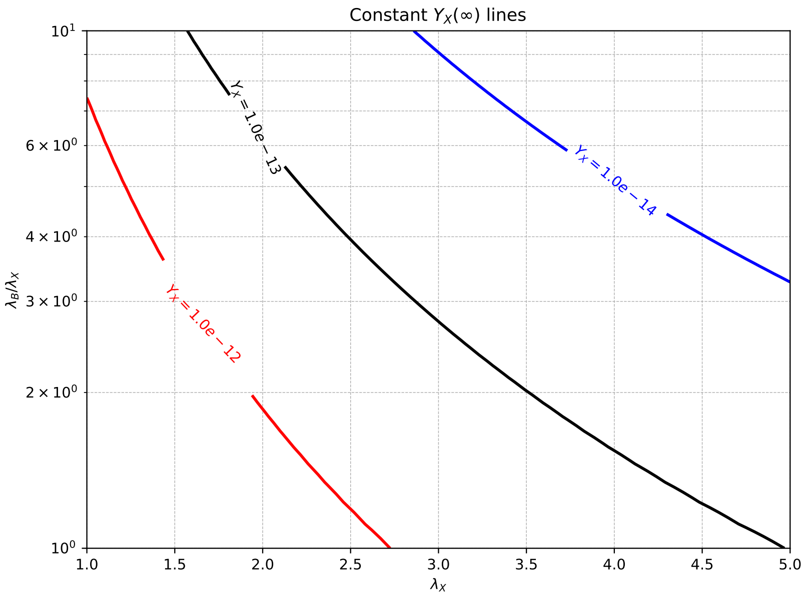

Figure 4.5: Contour plot showing the final comoving abundance Y_X as a function of the coupling λ_X and the ratio λ_B/λ_X, keeping the masses fixed at $m_X = 4.25$ TeV, $m_\Psi = 7.25$ TeV, $m_S = 5$ TeV. The observed value $Y_X^{\text{obs}} = 9.98 \times 10^{-14}$ (from $\Omega_X h^2 \sim 0.12$) is represented in black, while the red and blue contour lines represent, respectively, an arbitrary upper and lower bound to the relic WIMPs density, which helps for the identification of the viable parameter region.

stops and stabilizes to the value that is observed today.

For all the results shown, the parameter $n = 0$ has been adopted in the analytical terms, corresponding to assuming the thermally averaged cross-section to be independent from the velocity. This choice allows to capture the essential features of the physical processes, however, for a more detailed treatment, this assumption could be relaxed considering higher order terms.

These numerical results thus serve to illustrate the internal consistency of the model, and to highlight how different parameter choices affect the outcome of the asymmetry. A full derivation of the cross-sections and technical details involved in the numerical implementation is provided in Appendix C.

[11]The result is to be interpreted qualitatively, as the approximation used does not strictly enforce the parameter constraints derived from the relic abundance isolines. Nevertheless, the evolution illustrates the mechanism of asymmetry generation and freeze-out.

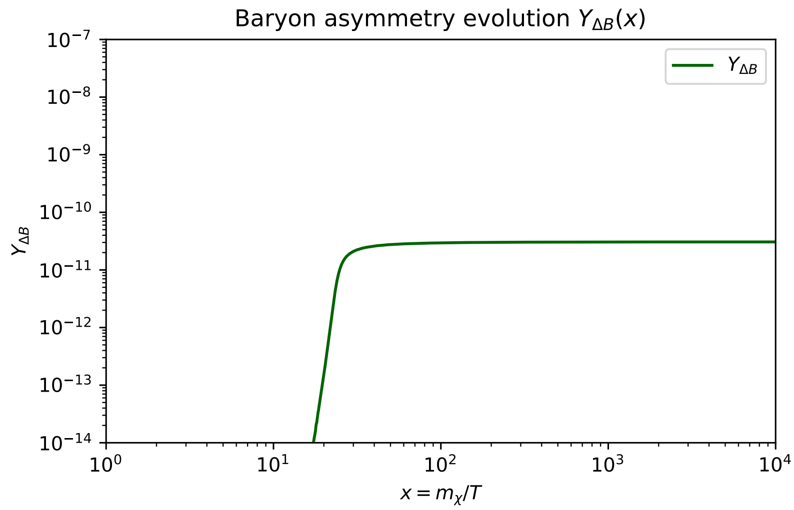

Figure 4.6: Evolution of the baryon asymmetry $Y_{\Delta B}$ as derived from the approximate equation 4.32. The parameters used in this plot are: $m_X = 4$ TeV, $m_\Psi = 7.5$ TeV, $m_S = 5$ TeV, $\lambda_X = 2$, $\lambda_B = 2.5$, $|\epsilon| = 0.25$. The resulting annihilation cross-section is $\sigma_{\text{ann}} = 1.02 \times 10^{-11}\text{GeV}^{-2}$, while the washout cross-section used, estimated under some approximations, is $\sigma_{\text{wa}} = 3.74 \times 10^{-9}\text{GeV}^{-2}$. The annihilations freeze-out temperature corresponds to $x_f \sim 21$. With these parameters, the integration of the Boltzmann equation gives as estimate of the final baryon asymmetry density $Y_{\Delta B}(\infty) \simeq 3.06 \times 10^{-11}$, which corresponds to a baryon-to-photon ratio $\eta \simeq 2.16 \times 10^{-10}$ - the same order of magnitude of the observed value[11].

5

Conclusions and Future Works

The work developed in this thesis has been devoted to the possibility of addressing two fundamental open problems in cosmology - dark matter and the baryon asymmetry of the Universe - through a unified mechanism. Beginning with a discussion on the limitations of the Standard Model, we focused on the theoretical requirements for baryogenesis and on Weakly Interacting Massive Particles (WIMPs) as dark matter candidates. This set the stage for the analysis of WIMPy baryogenesis, a scenario in which the annihilation of WIMPs itself is responsible for generating the baryon asymmetry while naturally explaining the relic abundance of dark matter.

Particular emphasis was placed on a specific realization of this mechanism, in which WIMPs annihilate directly into Standard Model quarks and a heavy exotic baryon-number carrying field. Through the construction and analysis of Boltzmann equations, the evolution of both the dark matter and baryon number densities was tracked, revealing key dependencies on the model' s parameters (most notably, the mass hierarchy between dark matter and the exotic field).

The central finding from this model is that a successful generation of the observed baryon asymmetry is contingent upon the freeze-out of washout processes occurring before the dark matter annihilations freeze-out. This requires a specific mass configuration: the exotic baryon must be heavier than the dark matter particle but lighter than twice its mass. In this mass window, washout scatterings become Boltzmann-suppressed early enough to allow WIMP annihilations to efficiently produce a net baryon number. Crucially, WIMPy baryogenesis is based on the fact that WIMPs annihilations in the early universe can satisfy all Sakharov conditions for baryogenesis if they occur violating CP and B in the Standard Model. Also, a preserved discrete symmetry is introduced to protect the generated asymmetry from washout, which prevents some decay channels of the exotic baryon into Standard Model fields. These theoretical ingredients ensure that the model is consistent and self-contained, making it a possible mechanism for baryogenesis at the weak scale.

From a phenomenological point of view, the model offers a number of testable implications. While the predicted baryon-to-dark matter ratio can vary within a broad range (about seven orders of magnitude) it can naturally accommodate the observed value. Furthermore, given that all relevant new particles are expected to lie at the weak scale, this framework is potentially within reach of current, or at least near-future, experiments. As outlined in [6], several experimental avenues are available.

For example, in terms of direct detection, dark matter scattering off nucleons would present a cross-section that is large enough to be detected in latest experiments, such as XENON1T. Being this cross-section suppressed by heavy-fields loops, a direct coupling of WIMPs with quarks is needed to provide a sufficiently high value, which excludes WIMPs annihilation channels to leptons as testable models through direct detection.

Since dark matter in the WIMPy baryogenesis model is expected to remain symmetric (i.e., both particles and antiparticles are present today), WIMP annihilations continue to occur at present time. This leads to the production of SM particles, including quarks, which hadronize giving signals of gamma rays, antiprotons, and anti-deuteron. Cosmic-ray experiments and observations from telescopes (e.g. Fermi-LAT) can thus place indirect detection limits on the WIMPs mass regions.

WIMPy baryogenesis predicts the existence of new charged fields which, if can be produced at colliders, might decay into SM quarks plus missing energy and leave a recognizable signal. In the context of supersymmetry researches, LHC constraints on new colored fields can apply also to our model. In particular, bounds on the masses of the gluino and squark in the presence of a massless neutralino can reflect in WIMPy baryogenesis bounds on the masses of the corresponding fields, which are ψ, $\tilde{d}$, and the massless singlet neutral fermion n, respectively. For both the decay channels we have proposed for ψ, the phenomenology is the same: the production of two jets and a singlet. Actual LHC running have set a bound that excludes models with $m_\psi \lesssim 2$TeV at

$\sqrt{s} \sim 13$TeV, and there is the possibility of new colored scalars discovery in the mass range of our interest.

WIMPy baryogenesis is not the only mechanism under investigation. Leptogenesis, for instance, remains a prominent alternative, where a lepton asymmetry generated at high scales is converted into a baryon asymmetry via sphaleron processes. However, as already mentioned, these models presents stronger experimental limits, making them harder to test (at least for the current and upcoming research projects), which makes direct baryogenesis a more promising target.

Looking ahead, several possible directions can be pursued to further develop and test this scenario. Alternative symmetry structures or coupling schemes could be explored, trying also for example to relax certain assumptions, or to embed the model within a broader theoretical framework (e.g. supersymmetry). With respect to this work, refinements to the Boltzmann analysis are possible to sharpen the phenomenological predictions. Additionally, exploring other annihilation channels or extending the model to include flavor effects could enrich the observable implications.

In conclusion, WIMPy baryogenesis represents a theoretically interesting mechanism that rests on an interplay of particle masses, cross sections, and thermal history features, while offering a promising direction for future research and experimental investigation.

A Standard Model of Cosmology

The Standard Cosmological Model, also known as the ΛCDM model, is the prevailing theoretical framework describing the evolution of the universe, combining general relativity with observational data to explain its composition, dynamics, and history.

A.1 Friedmann equations

Observations support the idea that our universe is homogeneous and isotropic on large scales, and under these assumptions the metric that best describes an expanding universe is the FRW metric:

$$ds^2 = dt^2 - R^2(t)\Big(\frac{dr^2}{1-kr^2} + r^2 d\theta^2 + r^2 sin^2\theta d\phi^2\Big) \tag{A.1}$$

where (r, θ, ϕ) are spherical comoving coordinates, R(t) is the cosmic scale factor, and k is the curvature parameter (it can be equal to +1, -1 or 0). The physical coordinates are recovered multiplying the comoving ones by the scale factor.

In order to describe the dynamics of the expanding universe it should be solved the Einstein's equations, which are given by:

$$R_{\mu\nu} - \frac{1}{2}g_{\mu\nu}R = 8\pi G T_{\mu\nu} + \Lambda g_{\mu\nu} \tag{A.2}$$

Here $R_{\mu\nu}$ is the Ricci tensor, i.e. the result of the contraction of the first and third index of the Riemann tensor

$$R^{\lambda}_{\sigma\mu\nu} = \partial_{\mu}\Gamma^{\lambda}_{\sigma\nu} - \partial_{\nu}\Gamma^{\lambda}_{\sigma\mu} + \Gamma^{\lambda}_{\mu\rho}\Gamma^{\rho}_{\nu\sigma} - \Gamma^{\lambda}_{\nu\rho}\Gamma^{\rho}_{\mu\sigma}, \tag{A.3}$$

with the Christoffel symbols corresponding to:

$$\Gamma^{\mu}_{\nu\lambda} = \frac{1}{2}g_{\mu\nu}\Big(\frac{\partial g_{\rho\nu}}{\partial x^{\lambda}} + \frac{\partial g_{\rho\lambda}}{\partial x^{\nu}} + \frac{\partial g_{\nu\lambda}}{\partial x^{\rho}}\Big). \tag{A.4}$$

$T_{\mu\nu}$ instead is the stress-energy tensor of a perfect fluid that respects the FRW metric:

$$T_{\mu\nu} = diag(\rho(t), -P(t), -P(t), -P(t))). \tag{A.5}$$

The Einstein's equations are derived from the variation w.r.t. the metric of the total action $S = S_{HE} + S_M$, where

$$S_{HE} = -\frac{1}{16\pi G}\int d^4x\sqrt{-g}(R + 2\Lambda) \tag{A.6}$$

is the Hilbert-Einstein gravitational action, and

$$S_M = \int d^4x\sqrt{-g}\mathcal{L}_M \tag{A.7}$$

is the action associated to all the other particles. The action principle states that $\delta S/\delta g_{\mu\nu} = 0$, and from it the Einstein's equations follow automatically.

From the (0,0) and (i,j) components of the Einstein equations, plus the conservation law $T^{\mu\nu}_{;\nu} = 0$, one can obtain the Friedmann equations:

$$\frac{\dot{R}^2}{R^2} = \frac{8\pi G}{3}\rho - \frac{k}{R^2} \tag{A.8}$$

$$\frac{\ddot{R}}{R} = -\frac{4\pi G}{3}(\rho + 3P) \tag{A.9}$$

$$\dot{\rho} + 3\frac{\dot{R}}{R}(\rho + P). \tag{A.10}$$

Only two of these equations are independent, so there is need to add an equation of state to solve the system for R(t), $\rho(t)$ and P(t). The simplest equation that can be chosen is

$$P = \omega\rho, \qquad \omega = const. \tag{A.11}$$

Solving the Friedmann equations it can be obtained the temporal evolution of the scale factor

$$R(t) \propto t^{\frac{2}{3(1+\omega)}} \tag{A.12}$$

and of the energy density

$$\rho(t) \propto R^{-3(1+\omega)}, \tag{A.13}$$

that for the main universe's components results:

- for radiation, $\omega = 1/3$: $\rho \propto R^{-4}$ (dominates the Universe at early times),
- for matter, $\omega = 0$: $\rho \propto R^{-3}$ (dominates the Universe after radiation epoch),
- for vacuum energy (Λ), $\omega = -1$: ρ remains constant during Universe expansion.

The expansion rate of the Universe is determined by the Hubble parameter $H \equiv \dot{R}/R$, that varies over time according to the relation $H(t) = \frac{2}{3(1+\omega)}t^{-1}$.

It is usually defined also an Hubble radius $R_c = c/H(t) = c\tau_H(t)$, where τ_H represents the characteristic time of expansion and is called Hubble time.

The present value of the expansion rate is the so-called Hubble constant, H_0, and its value is of order $\sim h \cdot 100$ km/s·Mpc, with $h \sim 0.7$.

It can be defined a critical energy density,

$$\rho_c = \frac{3H_0^2}{8\pi G}, \tag{A.14}$$

that corresponds to a flat universe (k=0), and a dimensionless density parameter

$$\Omega = \frac{\rho}{\rho_c}, \tag{A.15}$$

that is given by the sum the components of the universe. The first Friedmann equation can be rewritten as a function of this term:

$$\frac{k}{H^2R^2} = \Omega - 1, \tag{A.16}$$

hence the sign of Ω is related to curvature of the universe:

- $\Omega > 1 \longrightarrow$ closed

- $\Omega = 1 \longrightarrow$ flat
- $\Omega < 1 \longrightarrow$ open.

A.2 Equilibrium thermodynamics

For a dilute, weakly interacting gas of particles with g internal degrees of freedom, the following quantities are defined in terms of the phase space distribution function f:

- Number density $n = \frac{g}{(2\pi)^3} \int f(p) d^3p$
- Energy density $\rho = \frac{g}{(2\pi)^3} \int E(p) f(p) d^3p$
- Pressure $P = \frac{g}{(2\pi)^3} \int \frac{|\vec{p}|^2}{3E(p)} f(p) d^3p$

where $E = \sqrt{|\vec{p}|^2 + m^2}$ is the energy of a particle with momentum $\vec{p}$ and mass m.

If a species is in kinetic equilibrium, the distribution function $f(p)$ follows the Fermi-Dirac or Bose-Einstein statistics:

$$f(p) = \frac{1}{e^{(E-\mu)/T} \pm 1}, \tag{A.17}$$

with μ the chemical potential and the $\pm$ relative to fermions and bosons, respectively.

When particles are in chemical equilibrium, their chemical potentials satisfy relations dictated by reactions. For example, if a particle i is involved in a reaction with other species of the type $i + j \leftrightarrow k + l$, then, if there is chemical equilibrium, their chemical potentials are related as $\mu_i + \mu_j = \mu_k + \mu_l$.

In the relativistic limit ($T >> m$) the three quantities become:

$$n(T) = \begin{cases} gT^3 \frac{\zeta(3)}{\pi^2} & \text{bosons} \\ gT^3 \frac{\zeta(3)}{\pi^2} \frac{3}{4} & \text{fermions} \end{cases} \tag{A.18}$$

$$\rho(T) = \begin{cases} gT^4 \frac{\zeta(3)}{\pi^2} & \text{bosons} \\ gT^4 \frac{\pi^2}{30} \frac{7}{8} & \text{fermions} \end{cases} \tag{A.19}$$

$$P(T) = \frac{\rho}{3} \tag{A.20}$$

($\zeta(3)$ is the Riemann zeta function of (3)).

In the non relativistic limit ($T << m$), instead:

$$n(T) = g\left(\frac{mT}{2\pi}\right)^{3/2} e^{-(m-\mu)/T} \tag{A.21}$$

$$\rho(T) = mn(T) \tag{A.22}$$

$$P(T) = nT << \rho(T) \tag{A.23}$$

If we express the total energy density and pressure of all species in equilibrium in terms of the photon temperature T, including only the relativistic species in the sums, we get:

$$\rho_{tot} = g_*(T)\frac{\pi^2}{30}T^4 \tag{A.24}$$

$$P_{tot} = \frac{\rho_{tot}}{3} \tag{A.25}$$

where it has been defined the effective massless degrees of freedom:

$$g_*(T) = \sum_{i=\text{bosons}} g_i\left(\frac{T_i}{T}\right)^4 + \frac{7}{8}\sum_{i=\text{fermions}} g_i\left(\frac{T_i}{T}\right)^4. \tag{A.26}$$

Applying the second law of thermodynamics to a comoving volume element (V = R^3) in the expanding universe, the total entropy in the comoving volume

$$S = \frac{R^3(\rho + P)}{T} \tag{A.27}$$

is constant if there is thermal equilibrium, which makes it a very useful quantity in studying processes during the universe evolution. It is useful to define also the entropy density, $s = \dfrac{\rho + P}{T}$, that gets the main contribution from relativistic species and can be approximated to:

$$s = \frac{2\pi^2}{45} g_{*s} T^3, \tag{A.28}$$

where g_{*s} accounts for the contributions of relativistic particles and is equal to:

$$g_{*s}(T) = \sum_{i=\text{bosons}} g_i \left(\frac{T_i}{T}\right)^3 + \frac{7}{8} \sum_{i=\text{fermions}} g_i \left(\frac{T_i}{T}\right)^3. \tag{A.29}$$

For most of the universe's history, all particle species shared the same temperature, allowing g_{*s} to be substituted by g_*.

It can be observed that the entropy density is proportional to the number density of photons n_γ, providing a useful relation:

$$s = 1.88 g_{*s} n_\gamma. \tag{A.30}$$

The entropy conservation in a comoving volume means that:

$$sR^3 = \text{const.} \tag{A.31}$$

and so $g_{*s} \cdot T^3 \cdot R^3$ is conserved during expansion. As a result, the temperature evolves as $T \propto R^{-1}$ when g_{*s} is constant, but when a species become NR its entropy is transferred to the remaining relativistic particles, which brings to a slower decrease in the temperature (as can be inferred from the relation $T \propto R^{-1} g_{*s}^{-1/3}$).

Equation $A.31$ implies also that for a comoving volume element $V = R^3 \propto s^{-1}$, so the abundance of species in a comoving volume can be defined as:

$$N \equiv \frac{n}{s}, \tag{A.32}$$

which is a very useful quantity for the study of particle's number evolution and decoupling.

B

Boltzmann equations

The Boltzmann equations allow to study the evolution of phase space distribution functions $f(x^\mu, p^\mu)$ of a given species i, and are very useful when we deal with out of equilibrium conditions.

The general form is:

$$\hat{L}[f] = \hat{C}[f], \tag{B.1}$$

where $\hat{L}[f]$ and $\hat{C}[f]$ are the Liouville operator and the Collision operator, that accounts for all the possible interactions.

In the NR limit the Liouville operator has the following espression:

$$\hat{L}[f(\vec{x}, \vec{v})] = \frac{df(\vec{x}, \vec{v})}{dt} = \left(\frac{\partial}{\partial t} + \frac{\partial \vec{x}}{\partial t}\nabla_{\vec{x}} + \frac{\partial \vec{v}}{\partial t}\nabla_{\vec{v}}\right) f, \tag{B.2}$$

while in the relativistic generalization it becomes:

$$\hat{L} = p^\alpha \frac{\partial}{\partial x^\alpha} - \Gamma^\alpha_{\beta\gamma} p^\beta p^\gamma \frac{\partial}{\partial p^\alpha}. \tag{B.3}$$

In the FRW model we can simplify the equations applying the conditions of homogeneity and isotropy ($f(x^\alpha, p^\alpha) = f(E, t)$); this leads to the form:

$$E\frac{\partial f}{\partial t} - Hp^2 \frac{\partial f}{\partial E} = \hat{C}[f]. \tag{B.4}$$

This equation can be further rewritten, recalling the number density definition $n(t) = \frac{g}{(2\pi)^3}\int d^3p f(p, t)$, and after some manipulation and integration by parts we obtain:

$$\dot{n}(t) + 3Hn(t) = \frac{g}{(2\pi)^3}\int d^3p\,\frac{\hat{C}}{E}. \tag{B.5}$$

If we take for example a process: $1 + 2 \longleftrightarrow 3 + 4$, and we are interested in the evolution of the number density of particle 1, n_1, the collision term explicit form is:

$$\begin{aligned} &-\int d\Pi_1 d\Pi_2 d\Pi_3 d\Pi_4 (2\pi)^4 \delta^4(p_1 + p_2 - p_3 - p_4)\cdot \\ &\cdot \left[|M_{1+2\to3+4}|^2 f_1 f_2 (1 \pm f_3)(1 \pm f_4) - |M_{3+4\to1+2}|^2 f_3 f_4 (1 \pm f_1)(1 \pm f_2)\right] \end{aligned} \tag{B.6}$$

where the terms $(1 \pm f_i)$ are Bose enhancement factors (+) and Pauli blocking terms (-), the delta function implements the conservation of energy and momentum and $d\Pi_i = \frac{g_i d^3 p_i}{(2\pi)^3 2E_i}$.

It can be applied a simplification to this equation, that is valid in absence of degenerate Fermi species and Bose condensate, substituting the Maxwell-Boltzmann statistic to the Fermi-Dirac and Bose Einstein ones. In this approximation the terms $(1 \pm f_i)$ become of order 1, and, for all the species that are in kinetic equilibrium, the distribution functions take the form:

$$f_i(E_i) = e^{-\frac{E_i - \mu_i}{T}}. \tag{B.7}$$

The Boltzmann equation after this consideration becomes:

$$\begin{aligned} \dot{n}_1(t) + 3Hn_1(t) = &-\int d\Pi_1 d\Pi_2 d\Pi_3 d\Pi_4 (2\pi)^4 \delta^4(p_1 + p_2 - p_3 - p_4)\cdot \\ &\cdot \left[|M_{1+2\to3+4}|^2 f_1 f_2 - |M_{3+4\to1+2}|^2 f_3 f_4\right]. \end{aligned} \tag{B.8}$$

In the following parts two interesting cases will be studied: the Boltzmann equations for Baryogenesis and the Boltzmann equations for WIMPs models. Eventually, it will be also analyzed the Boltzmann equations regarding the framework of greatest interest for this thesis: WIMPy Baryogenesis.

B.1 Boltzmann equations for Baryogenesis

For the baryogenesis purpose, we consider a simplified model that includes a massive boson $X = \bar{X}$ with interactions that violate B, C and CP, relativistic particles b and $\bar{b}$ carrying baryon numbers + 1/2 and - 1/2 respectively, and a thermal bath of relativistic particles, with g_* degrees of freedom and no baryon numbers.

The amplitudes for the processes of X decay are:

$$|M(X \to bb)|^2 = |M(\bar{b}\bar{b} \to X)|^2 = \frac{1}{2}(1+\epsilon)|M_0|^2 \tag{B.9}$$

$$|M(X \to \bar{b}\bar{b})|^2 = |M(bb \to X)|^2 = \frac{1}{2}(1-\epsilon)|M_0|^2 \tag{B.10}$$

where ϵ is the violation of baryon number for a single process.

If we assume kinetic equilibrium (X and $b, \bar{b}$ have rapid enough interactions with the plasma), $\mu_b = -\mu_{\bar{b}} \equiv \mu$, and we can write the phase space distribution functions as:

$$f_b(E) = e^{-\dfrac{E-\mu}{T}} \qquad f_{\bar{b}}(E) = e^{-\dfrac{E+\mu}{T}} \qquad f_X(E) = e^{-\dfrac{E-\mu_X}{T}} \tag{B.11}$$

Assuming also chemical equilibrium (meaning that decays are efficient) we would have that $\mu = \mu_X = 0$, which can be easily proved to provide a zero value for B, so we consider a situation with just kinetic and no thermal equilibrium.

With these premises, the Boltzmann equations for the number density of X are:

$$\begin{aligned} \dot{n}_X + 3Hn_X = \int d\Pi_X d\Pi_1 d\Pi_2 (2\pi)^4 \delta^4(p_X - p_1 - p_2)[-|M_0|^2 f_X(p_X) + \\ +\frac{1}{2}(1+\epsilon)|M_0|^2 f_{\bar{b}}(p_1) f_{\bar{b}}(p_2) + \frac{1}{2}(1-\epsilon)|M_0|^2 f_b(p_1) f_b(p_2)]. \end{aligned} \tag{B.12}$$

The distribution functions terms, applying $B.11$, can be rewritten:

$$f_b(p_1)f_b(p_2) = e^{-\dfrac{E_1+E_2}{T}} e^{\dfrac{2\mu}{T}} \simeq f_X^{eq}(p_X)\left(1+\frac{2\mu}{T}\right) \simeq f_X^{eq}(p_X)\left(1+\frac{2n_B}{n_\gamma}\right) \tag{B.13}$$

where in the last passage it has been used the relations:

$$n_b = n_b^{eq} e^{\mu/T} \simeq g_b T^3 e^{\mu/T} \simeq g_b n_\gamma e^{\mu/T} \tag{B.14}$$

$$B = \frac{n_B}{s} \approx \frac{1}{2} \frac{n_b - n_{\bar{b}}}{1.88 g *_s n_\gamma} \approx \frac{sinh(\mu/T)}{g*_s} \sim g *_s^{-1} \mu/T \tag{B.15}$$

so $B.12$ becomes:

$$\begin{aligned} \dot{n}_X + 3Hn_X = \int d\Pi_X d\Pi_1 d\Pi_2 (2\pi)^4 \delta^4(p_X - p_1 - p_2) \cdot \\ \cdot \Big[-|M_0|^2 f_X(p_X) + |M_0|^2 f_X^{eq}(p_X) + O\Big(\epsilon \frac{\mu}{T}\Big) \Big]. \end{aligned} \tag{B.16}$$

Recalling that $\frac{f_X}{f_X^{eq}} = \frac{n_X}{n_X^{eq}}$, and defining

$$\Gamma_D \equiv \frac{1}{n_X^{eq}} \int d\Pi_X d\Pi_1 d\Pi_2 (2\pi)^4 \delta^4(p_X - p_1 - p_2)[|M_0|^2 f_X^{eq}], \tag{B.17}$$

the Boltzmann equation can be simply expressed as:

$$\dot{n}_X + 3Hn_X = -\Gamma_D(n_X - n_X^{eq}). \tag{B.18}$$

The Boltzmann equations for the number density of baryons (and antibaryons), instead, will also account for processes $bb \leftrightarrow \bar{b}\bar{b}$. For baryons we have:

$$\begin{aligned} \dot{n}_b + 3Hn_b = \int d\Pi_X d\Pi_1 d\Pi_2 (2\pi)^4 \delta^4(p_X - p_1 - p_2) \cdot \\ \cdot [-(1-\epsilon)|M_0|^2 f_b(p_1) f_b(p_2) + (1+\epsilon)|M_0|^2 f_X(p_X)] + \\ + 2 \int d\Pi_1 d\Pi_2 d\Pi_3 d\Pi_4 (2\pi)^4 \delta^4(p_1 + p_2 - p_3 - p_4) \cdot \\ \cdot [-|M'_{bb\to\bar{b}\bar{b}}|^2 f_b(p_1) f_b(p_2) + |M'_{\bar{b}\bar{b}\to bb}|^2 f_{\bar{b}}(p_3) f_{\bar{b}}(p_4)] \end{aligned} \tag{B.19}$$

and for antibaryons it is sufficient to substitute b with $\bar{b}$ and ϵ with -ϵ.

Taking the difference between these two equations, we can obtain a similar equation for the net baryon number density n_B:

$$\dot{n}_B + 3Hn_B = \epsilon\Gamma_D(n_X - n_X^{eq}) - \frac{n_X^{eq}}{n_\gamma}n_B\Gamma_D - n_B n_\gamma\langle\sigma|v|\rangle \tag{B.20}$$

where the quantity

$$\langle\sigma|v|\rangle = \int d\Pi_1 d\Pi_2 d\Pi_3 d\Pi_4 (2\pi)^4\delta^4(p_1+p_2-p_3-p_4)f_X^{eq}(p_X)|M'_{bb\to\bar{b}\bar{b}}|^2\frac{1}{n_\gamma^2} \propto$$
$$\propto \frac{\alpha^2 T^2}{(T^2+m_X^2)^2} \tag{B.21}$$

is the thermal averaged cross section of $2 \leftrightarrow 2$ B-nonconserving interactions. It can be observed that in the RHS of $B.20$ are present a source of baryon asymmetry that depends on the three Sakharov conditions (the first term is different from zero only if $n_X \neq n_X^{eq}$), and two terms that dampen the asymmetry accounting for inverse decays and $2 \leftrightarrow 2$ B-nonconserving interactions.

Together with $B.18$, $B.20$ forms a system of equations that can be solved for the evolution of B. These two equations can be transformed introducing the comoving quantities $X = \frac{n_X}{s}$ and $B = \frac{n_B}{s}$, and using the time variable $x = \frac{m_X}{T}$:

- the LHS of $B.18$ can be rewritten as: $\dot{n}_X + 3Hn_X = s\dot{X}$, and then we can transform the time derivative into a derivative with respect to x, which allows us to write:

$$X' = -\frac{\Gamma_D}{xH}(X - X^{eq}) = -\frac{x\Gamma_D}{H(x=1)}(X - X^{eq}). \tag{B.22}$$

Now, defining $\Delta = X - X^{eq}$, the equation can finally be expressed as:

$$\Delta' = -X'^{eq} - xK\gamma_D(x)\Delta(x) \tag{B.23}$$

where

$$\gamma_D(x) = \frac{\Gamma_D(x)}{\Gamma_D(x=1)} = \begin{cases} x & x << 1 \\ 1 & x >> 1 \end{cases} \tag{B.24}$$

and

$$X^{eq} = \frac{n_X^{eq}}{s} \simeq \begin{cases} g_*^{-1} & x << 1 \\ g_*^{-1} x^{3/2} e^{-x} & x >> 1 \end{cases}. \tag{B.25}$$

- It can be done the same thing for B, obtaining:

$$B' = \epsilon x K \gamma_D(x) \Delta - x K \gamma_B(x) B \tag{B.26}$$

where

$$\begin{aligned} \gamma_B(x) &\equiv (g_{*s} \gamma_D(x) X^{eq}(x) + 8 n_\gamma < \sigma |v| >) \frac{1}{\Gamma_D(x=1)} \simeq \\ &\simeq \begin{cases} x/2 + A\alpha/x & x << 1 \\ x^{3/2} e^{-x} + A\alpha x^{-5} & x >> 1 \end{cases} \end{aligned} \tag{B.27}$$

It is possible to integrate these two equations:

$$\begin{aligned} \Delta(x) = &\Delta_i exp\Big(\int_0^x -x' \gamma_D(x') K dx' \Big) - \\ &- \int_0^x X^{eq}(x') exp\Big(- \int_{x'}^x x'' K \gamma_D(x'') dx'' \Big) dx' \end{aligned} \tag{B.28}$$

$$\begin{aligned} B(x) = &B_i exp\Big(\int_0^{zx} -x' \gamma_B(x') K dx' \Big) + \\ &+ \epsilon K \int_0^x x' \gamma_D(x') \Delta(x') exp\Big(- \int_{x'}^x x'' K \gamma_B(x'') dx'' \Big) dx' \end{aligned} \tag{B.29}$$

and we take the initial departure from equilibrium Δ_i and the initial baryon asymmetry B_i to be zero, so the equations simplify a lot.

Now we want to study the solutions in different regimes, starting from K«1 (out of equilibrium decays). In this limit the solution of the first equation of the system is:

$$\Delta(x) \simeq -[X^{eq}(x) - X^{eq}(0)] e^{-Kx^2/2} \tag{B.30}$$

which gives:

$$X(x) \simeq X^{eq}(0) e^{-Kx^2/2}. \tag{B.31}$$

This means that once X decoupled and then decays efficiently, n_X drops.

The solution of the second equation for K«1 is:

$$B(x) \simeq -\epsilon[X^{eq}(0)e^{-Kx^2/2} - X^{eq}(0)] \tag{B.32}$$

which gives a value of B today:

$$B_f = B(x >> 1) = \epsilon X^{eq}(x = 0) \simeq \frac{\epsilon}{g_*} \tag{B.33}$$

as expected from the simpler considerations made in section 2.2.3 of chapter 2 regarding Baryogenesis.

In the opposite limit, $K >> 1$, the X particles tend to follow the equilibrium value, so $\Delta'(x)$ can be taken to be ~ 0 and the solution of B.28 is immediate:

$$\Delta = -\frac{X'^{eq}(x)}{xK\gamma_D(x)} \simeq \frac{X^{eq}(x)}{xK\gamma_D(x)} \tag{B.34}$$

(we always focus on x»1), and this is valid also for K ≥ 1.

To solve the equation for B it can be used the Laplace method, and it results:

$$B_f \simeq \frac{\epsilon}{g_*} x_f^{3/2} e^{-x_f} \frac{1}{\sqrt{|(xK\gamma_B(x)'|\Big|_{x_f}}} \tag{B.35}$$

where x_f is such that $x_f K\gamma_B(x_f) = 1$, and represents the freeze-out epoch, at which the processes that tend to dump B become inefficient.

In the K ≥ 1 case, inverse decays are the dominant processes that dump B, therefore the condition $x_f K\gamma_B(x_f) \simeq 1$ is $x_f^{5/2} K e^{-x_f} \simeq 1$, that gives asymptotically $x_f \simeq lnK$, and more precisely, considering K smaller than a critical value, $x_f \simeq 4(lnK)^{0.6}$. Taking now the derivative and inserting it into B.35 it results:

$$B_f \simeq \frac{\epsilon}{g_* K x_f} \simeq \frac{\epsilon}{g_* K 4(lnK)^{0.6}} \tag{B.36}$$

and we can observe that for increasing K there is a suppression factor ($\sim 1/K$), but not so strong.

In the $K >> 1$ limit, instead, B is damped mainly by scattering processes, and the freeze-out condition is $A\alpha K x_f^{-4} \simeq 1$, hence $x_f \simeq (A\alpha K)^{1/4}$. The baryon number, here, becomes:

$$B_f \simeq \frac{\epsilon}{g_*} x_f^2 e^{-x_f} \simeq \frac{\epsilon}{g_*} (A\alpha K)^{1/2} e^{-(A\alpha K)^{1/4}} \tag{B.37}$$

and in this case we observe an exponential suppression.

The comparison between the development of the baryon asymmetry B as a function of x for the three different regimes of K is displayed in fig. $B.1$. The critical value K_C is found imposing $x_f^{Scatt} \simeq x_f^{I.D.}$ and defines the boundary below which scattering processes become inefficient earlier than inverse decays and above which it's the opposite.

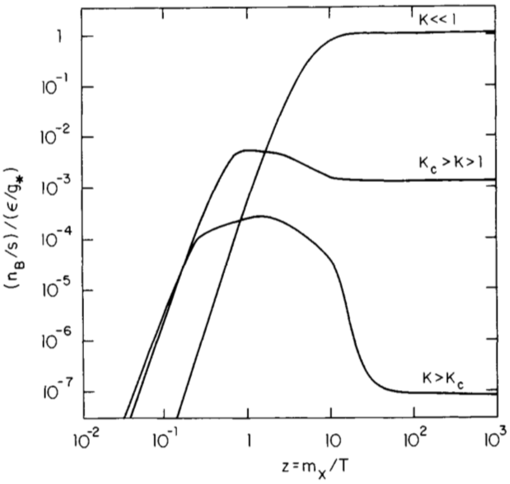

Figure B.1: Results of numerical integration of the equations for the evolution of the baryon asymmetry, in the three regimes K«1, K_C>K>1 and K»K_C, as function of $z = m_X/T$ [10].

B.2 Boltzmann equations for WIMPs

WIMPs species, that will be denoted as Ψ, are considered to be stable and interacting with other species X only through annihilations and inverse annihilations:

$$\Psi\bar{\Psi} \longleftrightarrow X\bar{X}, \tag{B.38}$$

which are the only processes responsible for variation in their number density. X are considered in thermal equilibrium with the plasma (since they undergo other stronger interactions), so $\mu_X = 0$, and $n_\Psi = n_{\bar{\Psi}}$, $n_X = n_{\bar{X}}$ (there is no asymmetry).

We can now work on equation $B.8$, considering the factors $f_\Psi f_{\bar{\Psi}}$ and $f_X f_{\bar{X}}$:

$$f_X(E_X) = e^{-\dfrac{E_X}{T}} \qquad f_{\bar{X}}(E_{\bar{X}}) = e^{-\dfrac{E_{\bar{X}}}{T}} \tag{B.39}$$

that, applying energy conservation and the fact that $f_\Psi^{eq} = e^{-\dfrac{E_\Psi}{T}}$, $f_{\bar{\Psi}}^{eq} = e^{-\dfrac{E_{\bar{\Psi}}}{T}}$, can be written as:

$$f_X f_{\bar{X}} = e^{-\dfrac{E_X + E_{\bar{X}}}{T}} = e^{-\dfrac{E_\Psi + E_{\bar{\Psi}}}{T}} = f_\Psi^{eq} f_{\bar{\Psi}}^{eq}. \tag{B.40}$$

Another simplification to equation $B.8$ can be done if we assume time reversal symmetry, which allows to write:

$$|M_{\Psi\bar{\Psi}\to X\bar{X}}|^2 = |M_{X\bar{X}\to\Psi\bar{\Psi}}|^2 \equiv |M|^2. \tag{B.41}$$

The Boltzmann equation becomes:

$$\begin{aligned} \dot{n_\Psi}(t) + 3Hn_\Psi(t) = -\int d\Pi_\Psi d\Pi_{\bar{\Psi}} d\Pi_X d\Pi_{\bar{X}} (2\pi)^4 \delta^4(p_\Psi + p_{\bar{\Psi}} - p_X - p_{\bar{X}}) \cdot \\ \cdot |M|^2 [f_\Psi^{eq} f_{\bar{\Psi}}^{eq} - f_\Psi f_{\bar{\Psi}}]. \end{aligned} \tag{B.42}$$

It can be followed now the same procedure used in the previous section: recalling that $\frac{f_\Psi}{f_\Psi^{eq}} = \frac{n_\Psi}{n_\Psi^{eq}}$, and defining

$$\langle\sigma|v|\rangle \equiv \frac{1}{n_\Psi^{2\,eq}} \int d\Pi_\Psi d\Pi_{\bar{\Psi}} d\Pi_X d\Pi_{\bar{X}} (2\pi)^4 \delta^4(p_\Psi + p_{\bar{\Psi}} - p_X - p_{\bar{X}}) |M|^2 f_\Psi^{eq} f_{\bar{\Psi}}^{eq}, \tag{B.43}$$

the Boltzmann equation can be simply expressed as:

$$\dot{n}_\Psi + 3Hn_\Psi = -\langle\sigma|v|\rangle(n_\Psi^2 - n_\Psi^{2\,eq}), \tag{B.44}$$

where the thermally-averaged annihilation cross section times velocity should include all annihilations channels.

B.3 Boltzmann equations for WIMPy Baryogenesis

The WIMP species will be here denoted by X, while barions and antibarions with b and $\bar{b}$.

The processes that dominate the evolution of the number density of WIMPs are annihilations and anti-annihilations of dark matter into (anti)baryons. Similarly to what was done in the previous computations, the amplitudes for these X annihilation processes can be expressed as:

$$|M(XX \to b)|^2 = |M(\bar{b} \to XX)|^2 = \left(1 + \frac{\epsilon}{2}\right)|M_{ann}|^2 \tag{B.45}$$

$$|M(XX \to \bar{b})|^2 = |M(b \to XX)|^2 = \left(1 - \frac{\epsilon}{2}\right)|M_{ann}|^2 \tag{B.46}$$

where ϵ is the baryon number violation corresponding to each WIMPs annihilation.

The Boltzmann equation for the WIMPs number density is then:

$$\begin{aligned}\dot{n}_X + 3Hn_X = &\int d\Pi_1 d\Pi_2 d\Pi_b (2\pi)^4 \delta^4(p_1 + p_2 - p_b)\cdot \\ &\cdot\left[-\left(1+\frac{\epsilon}{2}\right)|M_{ann}|^2 f_X(p_1) f_X(p_2) + \left(1-\frac{\epsilon}{2}\right)|M_{ann}|^2 f_b(p_b)\right] + \\ &+ \int d\Pi_1 d\Pi_2 d\Pi_{\bar{b}} (2\pi)^4 \delta^4(p_1 + p_2 - p_{\bar{b}})\cdot \\ &\cdot\left[-\left(1+\frac{\epsilon}{2}\right)|M_{ann}|^2 f_X(p_1) f_X(p_2) + \left(1+\frac{\epsilon}{2}\right)|M_{ann}|^2 f_{\bar{b}}(p_{\bar{b}})\right].\end{aligned} \tag{B.47}$$

Recalling the considerations we did about baryogenesis in section $B.1$, the distribution functions of baryons and antibaryons can be rewritten as:

$$f_b(p_b) = e^{-\frac{E_b}{T}} e^{\frac{\mu}{T}} = e^{-\frac{E_1+E_2}{T}} e^{\frac{\mu}{T}} \simeq f_X^{eq}(p_1) f_X^{eq}(p_2)\left(1 + \frac{\mu}{T}\right) \tag{B.48}$$

$$f_{\bar{b}}(p_{\bar{b}}) = e^{-\frac{E_{\bar{b}}}{T}} e^{-\frac{\mu}{T}} = e^{-\frac{E_1+E_2}{T}} e^{-\frac{\mu}{T}} \simeq f_X^{eq}(p_1) f_X^{eq}(p_2)\left(1 - \frac{\mu}{T}\right) \tag{B.49}$$

and applying these to equation $B.47$ we can follow the same procedure that was displayed in the previous sections to finally express the Boltzmann equation in the simple form:

$$\dot{n}_X + 3Hn_X = -2\langle\sigma_{ann}|v|\rangle(n_X^2 - (n_X^{eq})^2), \tag{B.50}$$

where it has been defined the annihilation cross section as:

$$\langle\sigma_{ann}|v|\rangle \equiv \frac{1}{(n_X^{eq})^2}\int d\Pi_1 d\Pi_2 d\Pi_b (2\pi)^4\delta^4(p_1+p_2-p_b)[|M_{ann}|^2 f_X^{eq}(p_1) f_X^{eq}(p_2)]. \tag{B.51}$$

Writing the equation as function of the usual dimensionless variables $Y_X = n_X/s$ and $x = m_X/T$, it results:

$$\frac{dY_X}{dx} = -\frac{2s(x)\langle\sigma_{ann}|v|\rangle}{xH(x)}(Y_X^2 - (Y_X^{eq})^2). \tag{B.52}$$

Considering now the baryon asymmetry evolution, we should proceed following the same steps that have been presented in section $B.1$: once we find the Boltzmann equations for baryons and antibaryons, they should be subtracted to obtain the Boltzmann equation for the net B.

In addition to annihilations and anti-annihilations of WIMPs, other interactions that modify the baryon number density are the baryon - antibaryon scatterings, that act as washout processes, and for the purpose of a general treatment without entering in details they will be here represented by $b \leftrightarrow \bar{b}$. The Boltzmann equation for baryons is then:

$$\begin{aligned}\dot{n}_b + 3Hn_b = &\int d\Pi_b d\Pi_1 d\Pi_2 (2\pi)^4\delta^4(p_b - p_1 - p_2)\cdot\\ &\cdot\Big[+\Big(1+\frac{\epsilon}{2}\Big)|M_{ann}|^2 f_X(p_1) f_X(p_2) - \Big(1-\frac{\epsilon}{2}\Big)|M_{ann}|^2 f_b(p_b)\Big] +\\ &+2\int d\Pi_b d\Pi_{\bar{b}}(2\pi)^4\delta^4(p_b - p_{\bar{b}})[-|M'_{b\to\bar{b}}|^2 f_b(p_b) + |M'_{\bar{b}\to b}|^2 f_{\bar{b}}(p_{\bar{b}})],\end{aligned} \tag{B.53}$$

and the corresponding equation for antibaryons, as already seen, can be obtained by substitution of b with $\bar{b}$ and of ϵ with $-\epsilon$.

When we compute the Boltzmann equation for the net ΔB, subtracting the equation for $\bar{b}$ from $B.53$, we do the same simplifications that has been adopted in the previous calculations, and we neglect terms of order $O\Big(\epsilon\frac{\mu}{T}\Big)$. The procedure is very similar to what is explained in [10] regarding generic Baryogenesis.

From the first part of the equations and the CP-nonconserving contribution of the second part ($|M'_{b\to\bar{b}}|^2 \neq |M'_{\bar{b}\to b}|^2$) it can be obtained a term proportional to the annihilation rate of X (B.50) multiplied by the fractional asymmetry ϵ. Similarly to what we found in $B.20$ for the case of Baryogenesis by decay of a particle X, there are also two terms that tend to dampen the baryon asymmetry, one coming from the (anti)annihilation processes, and another coming from the baryon-antibaryon scatterings[1]. In practice, the resulting equation is:

$$\dot{n}_{\Delta B} + 3Hn_{\Delta B} = \epsilon\langle\sigma_{ann}|v|\rangle(n_X^2 - (n_X^{eq})^2) - 2\frac{\mu}{T}\langle\sigma_{ann}|v|\rangle(n_X^{eq})^2 - 4\frac{\mu}{T}\langle\sigma_{wa}|v|\rangle n_b^{eq} n_{\bar{b}}^{eq}, \tag{B.54}$$

where it has been defined a cross section for the washout processes[2]:

$$\begin{aligned}\langle\sigma_{ann}|v|\rangle \equiv &\frac{1}{n_b^{eq} n_{\bar{b}}^{eq}} \int d\Pi_1 d\Pi_2 d\Pi_b d\Pi_{\bar{b}} (2\pi)^4 \delta^4(p_1 + p_2 - p_b - p_{\bar{b}}) \cdot \\ &\cdot [|M_{wa}|^2 f_X^{eq}(p_1) f_X^{eq}(p_2)].\end{aligned} \tag{B.55}$$

If we take into account the two terms responsible for the washout of the baryon asymmetry, we can notice that the first one, which is caused by WIMPs anti-annihilations and is proportional to $(n_X^{eq})^2$, is Boltzmann-suppressed for $x > 1$ (the thermal baryons have not anymore energy to anti-annihilate into WIMPs). This term for this reason can be neglected with respect to the other stronger contribution from baryons-antibaryons scatterings.

What results, using the dimensionless variables, is:

$$\frac{dY_{\Delta B}}{dx} = \frac{\epsilon\, s(x)}{x\, H(x)} \langle\sigma_{ann}|v|\rangle(Y_X^2 - (Y_X^{\text{eq}})^2) - \frac{s(x)}{x\, H(x)} \langle\sigma_{wa}|v|\rangle \frac{\mu}{T} \prod_i Y_i^{eq}, \tag{B.56}$$

where the Y_i account for the exact baryon states that are taking part in the washout scattering processes.

[1]This term derives from the CP-conserving contribution of the second part of the Boltzmann equation, that satisfies the condition $|M'_{b\to\bar{b}}|^2 = |M'_{\bar{b}\to b}|^2$

[2]The matrix element is here defined as $|M_{wa}|^2 \equiv |M'_{b\to\bar{b}}|^2 = |M'_{\bar{b}\to b}|^2$, since it comes from the CP-conserving term

C

Cross Section Evaluation

C.1 WIMPs annihilation cross section

We consider the process of XX annihilation into a quark and an exotic baryon ψ, mediated by a scalar S, as in figure 4.2 (we consider the first diagram, tree level) with the interaction Lagrangian described by equation 4.22. We call the incoming particles momenta p_1 and p_2, while the momenta of the quark and of the baryon ψ are named, respectively, k_1 and k_2.

The matrix element is given by:

$$i\mathcal{M} = i\lambda_X \bar{v}_X(p_2) u_X(p_1) \cdot \frac{i}{s - m_S^2 + i m_S \Gamma_S} \cdot i\lambda_B \bar{u}_u(k_1) v_\psi(k_2). \tag{C.1}$$

We can write the amplitude squared: summing over spins we use the completeness relations

$$\sum_{i=1,2} u^{(i)} \bar{u}^{(i)} = \not{p} + m, \qquad \sum_{i=1,2} v^{(i)} \bar{v}^{(i)} = \not{p} - m \tag{C.2}$$

and, multiplying by the number of color states, we obtain:

$$|\mathcal{M}|^2 = \frac{3}{4} \frac{\lambda_X^2 \lambda_B^2}{(s - m_S^2)^2 + (m_S \Gamma_S)^2} \cdot \mathrm{Tr}[(\not{p}_2 - m_X)(\not{p}_1 + m_X)] \cdot \mathrm{Tr}[(\not{k}_1 + m_u)(\not{k}_2 - m_\psi)] \tag{C.3}$$

Applying the standard identities

$$\begin{aligned} \mathrm{Tr}[\text{odd number of } \gamma^\mu] = 0, \quad \mathrm{Tr}[\gamma^\mu\gamma^\nu] = 4\eta^{\mu\nu}, \\ \mathrm{Tr}[\gamma^\mu\gamma^\nu\gamma^\rho\gamma^\sigma] = 4(\eta^{\mu\nu}\eta^{\rho\sigma} - \eta^{\mu\rho}\eta^{\nu\sigma} + \eta^{\mu\sigma}\eta^{\nu\rho}), \end{aligned} \tag{C.4}$$

we can evaluate the traces in the amplitude squared:

$$\begin{aligned} &\mathrm{Tr}[(\not{p}_2 - m_X)(\not{p}_1 + m_X)] \cdot \mathrm{Tr}[(\not{k}_1 + m_u)(\not{k}_2 - m_\psi)] = \\ &= \mathrm{Tr}[(p_{2\mu}\gamma^\mu - m_X)(p_{1\nu}\gamma^\nu + m_X)] \cdot \mathrm{Tr}[(k_{1\alpha}\gamma^\alpha + m_u)(k_{2\beta}\gamma^\beta - m_\psi)] = \\ &= 4(p_2 \cdot p_1 - m_X^2) \cdot 4(k_1 \cdot k_2 - m_u m_\psi). \end{aligned} \tag{C.5}$$

This term can be rewritten as a function of the Mandelstam variable s and the masses using the relations:

$$s = (p_1 + p_2)^2 = (k_1 + k_2)^2, \quad \Rightarrow p_1 \cdot p_2 = \frac{s - 2m_X^2}{2} \quad k_1 \cdot k_2 = \frac{s - m_u^2 - m_\psi^2}{2}; \tag{C.6}$$

then, substituting:

$$|\mathcal{M}|^2 = 3\lambda_X^2\lambda_B^2 \frac{(s - 4m_X^2)(s - (m_u + m_\psi)^2)}{(s - m_S^2)^2 + (m_S\Gamma_S)^2} \tag{C.7}$$

We can finally find the cross section, which general formula is:

$$\sigma = \frac{1}{64\pi^2 s} \frac{|\vec{k}_f|}{|\vec{p}_i|} \int d\Omega \, |\mathcal{M}|^2. \tag{C.8}$$

The magnitudes of the initial and final momenta in the center of mass frame are:

$$|\vec{p}_i| = \frac{\sqrt{s - 4m_X^2}}{2}, \quad |\vec{k}_f| = \frac{1}{2\sqrt{s}} \sqrt{\lambda(s, m_u, m_\psi)}, \tag{C.9}$$

where λ is the Källén function:

$$\lambda(s, m_u, m_\psi) = s^2 + m_u^2 + m_\psi^2 - 2sm_u - 2sm_\psi - 2m_u m_\psi. \tag{C.10}$$

Substituting everything and integrating over solid angle we reach the final cross section formula, used in the computations of this thesis work:

$$\sigma = \frac{1}{16\pi s} \frac{\sqrt{\lambda(s, m_u, m_\psi)}}{\sqrt{s}\sqrt{s - 4m_X^2}} \cdot 3\lambda_X^2 \lambda_B^2 \frac{(s - 4m_X^2)(s - (m_u + m_\psi)^2)}{(s - m_S^2)^2 + (m_S \Gamma_S)^2} \tag{C.11}$$

In this situation we expect the center of mass energy to be $E_{\mathrm{CM}} = 2E_X \approx 2m_X$; for the calculations we assume it to be slightly above threshold, defining $s = 4m_X^2(1 + \epsilon)$, with $\epsilon = 0.01$.

C.2 Scattering cross-section

We now take into account the baryon-number washout process of scattering mediated by the scalar S, described by the Feynman diagrams in figure 4.3. The momenta of the quark and exotic baryon incoming fields are referred to as p_1 and p_2, while the momenta of the outgoing exotic baryon and quark are referred to as p_3 and p_4, respectively. Here we have explicitly written the spin indices for the each particle (s_1, s_2, r_1, r_2) and the spinor indices (a, b, c, d).

The matrix elements for the two channels are:

- S-channel:

$$i\mathcal{M}_s = i\lambda_B \bar{v}_a^{s_2}(p_2) u_a^{s_1}(p_1) \cdot \frac{i}{s - m_S^2 + i m_S \Gamma_S} \cdot i\lambda_B \bar{u}_b^{r_1}(p_3) v_b^{r_2}(p_4), \tag{C.12}$$

  where $s = (p_1 + p_2)^2$,

- T-channel:

$$i\mathcal{M}_t = i\lambda_B \bar{u}_c^{r_1}(p_3) u_c^{s_1}(p_1) \cdot \frac{i}{t - m_s^2} \cdot i\lambda_B \bar{v}_d^{s_2}(p_2) v_d^{r_2}(p_4), \tag{C.13}$$

  where $t = (p_1 - p_3)^2$,

and we can express the amplitude squared as:

$$|\mathcal{M}|^2 = |\mathcal{M}_s + \mathcal{M}_t|^2 = |\mathcal{M}_s|^2 + |\mathcal{M}_t|^2 + 2\Re(\mathcal{M}_s \mathcal{M}_t^*) \tag{C.14}$$

We now follow a similar procedure to the one used in the previous section, for the computation of the WIMPs annihilation cross-section:

- For the s-channel:

  Summing over spins and multiplying by the number of color states:

$$
\begin{aligned}
|\mathcal{M}_s|^2 &= \frac{3\lambda_B^4}{4} \frac{\mathrm{Tr}[(\not{p}_2 - m_\psi)(\not{p}_1 + m_u)] \cdot \mathrm{Tr}[(\not{p}_3 + m_\Psi)(\not{p}_4 - m_u)]}{(s - m_S^2)^2 + (m_S \Gamma_S)^2} = \\
&= \frac{3\lambda_B^4}{4} \frac{4(p_1 \cdot p_2 - m_\psi m_u) \cdot 4(p_3 \cdot p_4 - m_\psi m_u)}{(s - m_S^2)^2 + (m_S \Gamma_S)^2},
\end{aligned} \tag{C.15}
$$

  and applying the relations

$$
p_1 \cdot p_2 = \frac{s - m_u^2 - m_\Psi^2}{2} = p_3 \cdot p_4 \tag{C.16}
$$

  we can express the amplitude squared as:

$$
|\mathcal{M}_s|^2 = 3\lambda_B^4 \frac{\left(s - m_u^2 - m_\psi^2 - 2m_u m_\psi\right)^2}{(s - m_S^2)^2 + (m_S \Gamma_S)^2}. \tag{C.17}
$$

- For the t-channel:

$$
\begin{aligned}
|\mathcal{M}_s|^2 &= \frac{3}{4} \frac{\lambda_B^4}{(t - m_s^2)^2} \cdot \mathrm{Tr}[(\not{p}_1 + m_u)(\not{p}_3 + m_\psi)] \cdot \mathrm{Tr}[(\not{p}_2 - m_\psi)(\not{p}_4 - m_u] = \\
&= \frac{3}{4} \frac{\lambda_B^4}{(t - m_s^2)^2} \cdot 4(p_1 \cdot p_3 + m_u m_\psi) \cdot 4(p_2 \cdot p_4 + m_u m_\psi).
\end{aligned} \tag{C.18}
$$

  Using the definition of t we can obtain the relations:

$$
p_1 \cdot p_3 = \frac{m_u^2 + m_\psi^2 - t}{2} = p_2 \cdot p_4 \tag{C.19}
$$

  and $|\mathcal{M}_t|^2$ can be written as:

$$
|\mathcal{M}_t|^2 = 3\lambda_B^4 \frac{\left(m_u^2 + m_\psi^2 - t + 2m_u m_\psi\right)^2}{(t - m_s^2)^2}. \tag{C.20}
$$

  Considering the interaction in the center of mass frame, having the two initial particles the same momenta with opposite direction in the z-plane, the

4-momenta p_1 and p_3 are: $p_1 = (E_{\bar{u}}, 0, 0, |\vec{p}|)$, $p_3 = (E_\psi, |\vec{p}|sin\theta, 0, |\vec{p}|cos\theta)$, with θ the angle between the directions of p_1 and p_3 in a plane orthogonal to z. Thus, we can express t as a function of s by writing $t = m_u^2 + m_\psi^2 - 2p_1 \cdot p_3 = m_u^2 + m_\psi^2 - 2(E_u E_\psi - |\vec{p}|^2 \cos\theta)$, with $E_u = \dfrac{s + m_u^2 - m_\psi^2}{2\sqrt{s}}$, $E_\psi = \dfrac{s - m_u^2 + m_\psi^2}{2\sqrt{s}}$.

- For the interaction term between the s and t channels:

  The sum over spins gives:

$$\begin{aligned}\Re(\mathcal{M}_s \mathcal{M}_t^*) \propto &\frac{\lambda_B^4}{(s - m_S^2)(t - m_s^2)} \cdot \\ &\cdot \sum_{spins} [\bar{v}_a^{s_2}(p_2) u_a^{s_1}(p_1)][\bar{u}_b^{r_1}(p_3) v_b^{r_2}(p_4)][\bar{u}_c^{s_1}(p_1) u_c^{r_1}(p_3)][\bar{v}_d^{r_2}(p_4) v_d^{s_2}(p_2)]\end{aligned} \tag{C.21}$$

  and applying the completeness relations this can be rewritten as:

$$\Re(\mathcal{M}_s \mathcal{M}_t^*) \propto \frac{\lambda_B^4 \cdot \mathrm{Tr}[(\not{p}_2 - m_\psi)(\not{p}_1 + m_u)(\not{p}_3 + m_\Psi)(\not{p}_4 - m_u)]}{(s - m_S^2)(t - m_s^2)}. \tag{C.22}$$

  By expanding the products and applying the standard identities of the traces ($C.4$), it finally results:

$$\begin{aligned}\Re(\mathcal{M}_s \mathcal{M}_t^*) = &\frac{3\lambda_B^4}{(s - m_S^2)(t - m_s^2)} \cdot \\ &\cdot ((p_1 \cdot p_2)^2 - (p_1 \cdot p_3)^2 + (p_1 \cdot p_4)(p_2 \cdot p_3) - \\ &- 2m_\psi m_u (p_2 \cdot p_1) + 2m_u m_\psi (p_2 \cdot p_4) - (p_2 \cdot p_3) m_u^2 - (p_1 \cdot p_4) m_\psi^2 + m_u^2 m_\psi^2),\end{aligned} \tag{C.23}$$

  where we have taken into account the spin configurations and color factors, and we have applied the equalities $C.16$ and $C.19$. To compute the remaining products $(p_2 \cdot p_3)$ and $(p_1 \cdot p_4)$ we can use the Mandelstam variable $u = (p_2 - p_3)^2 = (p_1 - p_4)^2$, obtaining:

$$p_2 \cdot p_3 = \frac{2m_\psi^2 - u}{2}, \quad p_1 \cdot p_4 = \frac{2m_u^2 - u}{2}, \tag{C.24}$$

  where, similarly to t, the variable u can be expressed as $u = 2m_\psi^2 - 2p_2 \cdot p_3 =$

$2m_\psi^2 - 2(E_\psi^2 + |\vec{p}|^2 \cos\theta)$.

The second cross term, $\Re(\mathcal{M}_t \mathcal{M}_s^*)$, can be proved to be equal to $\Re(\mathcal{M}_s \mathcal{M}_t^*)$, so the overall interference term is accounted by $2\Re(\mathcal{M}_s \mathcal{M}_t^*)$.

Applying the general cross section formula $C.8$, the result is:

$$\begin{aligned}\sigma(s) =& \frac{1}{32\pi s}\frac{|\vec{p}_f|}{|\vec{p}_i|}\cdot \\ &\cdot\left(2|\mathcal{M}_s|^2 + \int_{-1}^{1}|\mathcal{M}_t(\cos\theta)|^2 dcos\theta + \int_{-1}^{1} 2\Re(\mathcal{M}_s \mathcal{M}_t^*)(\cos\theta) dcos\theta\right),\end{aligned} \tag{C.25}$$

where the initial and final momenta in the center of mass frame are given by $|\vec{p}_i| = |\vec{p}_f| = \dfrac{\sqrt{\lambda(s, m_u, m_\psi)}}{2\sqrt{s}}$.

References

[1] Gerard 't Hooft. "Renormalizable Lagrangians for Massive Yang-Mills Fields". In: *Nucl. Phys. B* 35 (1971). Ed. by J. C. Taylor, pp. 167–188. DOI: 10.1016/0550-3213(71)90139-8.

[2] G. Arnison et al. "Experimental Observation of Lepton Pairs of Invariant Mass Around 95-GeV/c**2 at the CERN SPS Collider". In: *Phys. Lett. B* 126 (1983), pp. 398–410. DOI: 10.1016/0370-2693(83)90188-0.

[3] Gianfranco Bertone, Dan Hooper, and Joseph Silk. "Particle dark matter: evidence, candidates and constraints". In: *Physics Reports* 405.56 (Jan. 2005), pp. 279–390. ISSN: 0370-1573. DOI: 10.1016/j.physrep.2004.08.031. URL: http://dx.doi.org/10.1016/j.physrep.2004.08.031.

[4] James M. Cline. *Baryogenesis*. 2006. arXiv: hep-ph/0609145 [hep-ph]. URL: https://arxiv.org/abs/hep-ph/0609145.

[5] James M. Cline. *TASI Lectures on Early Universe Cosmology: Inflation, Baryogenesis and Dark Matter*. 2021. arXiv: 1807.08749 [hep-ph]. URL: https://arxiv.org/abs/1807.08749.

[6] Yanou Cui, Lisa Randall, and Brian Shuve. "A WIMPy baryogenesis miracle". In: *Journal of High Energy Physics* 2012.4 (Apr. 2012). ISSN: 1029-8479. DOI: 10.1007/jhep04(2012)075. URL: http://dx.doi.org/10.1007/JHEP04(2012)075.

[7] Lorenzo Mai Giacomo Galloni and Leonardo Rebeschini. "Lecture Notes of Cosmology of the Early Universe". Lectures held by Professor Nicola Bartolo at Università degli Studi di Padova, Master Degree in Physics, Academic Year 2019-2020. 2020.

[8] F. J. Hasert et al. "Observation of Neutrino Like Interactions Without Muon Or Electron in the Gargamelle Neutrino Experiment". In: *Phys. Lett. B* 46 (1973), pp. 138–140. DOI: 10.1016/0370-2693(73)90499-1.

[9] M. J. Herrero. *The Standard Model*. 1998. arXiv: hep-ph/9812242 [hep-ph]. URL: https://arxiv.org/abs/hep-ph/9812242.

[10] Edward W. Kolb and Michael S. Turner. *The Early Universe*. Vol. 69. Taylor and Francis, May 2019. ISBN: 978-0-429-49286-0, 978-0-201-62674-2. DOI: 10.1201/9780429492860.

[11] E. Komatsu et al. "SEVEN-YEARWILKINSON MICROWAVE ANISOTROPY PROBE(WMAP) OBSERVATIONS: COSMOLOGICAL INTERPRETATION". In: *The Astrophysical Journal Supplement Series* 192.2 (Jan. 2011), p. 18. ISSN: 1538-4365. DOI: 10.1088/0067-0049/192/2/18. URL: http://dx.doi.org/10.1088/0067-0049/192/2/18.

[12] R. D. Peccei and Helen R. Quinn. "CP Conservation in the Presence of Pseudoparticles". In: *Phys. Rev. Lett.* 38 (25 June 1977), pp. 1440–1443. DOI: 10.1103/PhysRevLett.38.1440. URL: https://link.aps.org/doi/10.1103/PhysRevLett.38.1440.

[13] Mark Trodden. *Baryogenesis and Leptogenesis*. 2004. arXiv: hep-ph/0411301 [hep-ph]. URL: https://arxiv.org/abs/hep-ph/0411301.

[14] F. Zwicky. "Republication of: The redshift of extragalactic nebulae". In: *General Relativity and Gravitation* 41.1 (Jan. 2009), pp. 207–224. DOI: 10.1007/s10714-008-0707-4.